



HAL
open science

High-order finite elements in numerical electromagnetism: degrees of freedom and generators in duality

Marcella Bonazzoli, Francesca Rapetti

► **To cite this version:**

Marcella Bonazzoli, Francesca Rapetti. High-order finite elements in numerical electromagnetism: degrees of freedom and generators in duality. Numerical Algorithms, 2017, 10.1007/s11075-016-0141-8. hal-01260354

HAL Id: hal-01260354

<https://hal.science/hal-01260354>

Submitted on 2 Jun 2016

HAL is a multi-disciplinary open access archive for the deposit and dissemination of scientific research documents, whether they are published or not. The documents may come from teaching and research institutions in France or abroad, or from public or private research centers.

L'archive ouverte pluridisciplinaire **HAL**, est destinée au dépôt et à la diffusion de documents scientifiques de niveau recherche, publiés ou non, émanant des établissements d'enseignement et de recherche français ou étrangers, des laboratoires publics ou privés.

High order finite elements in numerical electromagnetism: degrees of freedom and generators in duality

Marcella Bonazzoli · Francesca Rapetti

Received: date / Accepted: date

Abstract Explicit generators for high order ($r > 1$) scalar and vector finite element spaces generally used in numerical electromagnetism are presented and classical degrees of freedom, the so-called moments, revisited. Properties of these generators on simplicial meshes are investigated and a general technique to restore duality between moments and generators is proposed. Algebraic and exponential optimal h - and r -error rates are numerically validated for high order edge elements on the problem of Maxwell's eigenvalues in a square domain.

Keywords High order FEs in electromagnetism, degrees of freedom and generators in duality, simplices

PACS 78M10 · 65N30 · 68U20

1 Introduction

When applying the finite element (FE) method to a given problem arising in science and engineering, one writes the weak formulation of the problem to be discretized, defines the suitable discrete FE space on a mesh covering the computational domain, and selects the algorithm to solve the final algebraic system in an efficient way [22]. For electromagnetic problems, one considers Maxwell's equations, which contain differential operators \mathcal{L} acting on scalar and vector fields such as the gradient, the curl and the divergence. To write the variational formulation of such equations, one introduces a

M. Bonazzoli and F. Rapetti
LJAD-Laboratoire de Mathématiques "J.A. Dieudonné", Université de Nice Sophia-Antipolis,
Parc Valrose, 06108 Nice, Cedex 02, France.
Tel.: +33-4-92076497
Fax: +33-4-93517974
E-mail: Marcella.BONAZZOLI@unice.fr, Francesca.RAPETTI@unice.fr

suitable functional space $H_{\mathcal{L}} = \{u \in L^2, \mathcal{L}u \in L^2\}$ for each of these operators. These spaces are linked by the operators to form a complex, that is, one defines the diagram $H_{grad} \xrightarrow{grad} H_{curl} \xrightarrow{curl} H_{div} \xrightarrow{div} L^2$ where the composition of two consecutive operators is 0. To define a correct discretization of the variational problem, one has to consider not only subspaces W_h^1 of H_{curl} but also subspaces W_h^0 of H_{grad} , W_h^2 of H_{div} and W_h^3 of L^2 , also forming for each h a complex for the same operators, being $h > 0$ the maximal diameter of the elements constituting a mesh τ_h over the computational domain, say Ω . It is also important to relate the two complexes by projections onto these subspaces, in order to form a diagram

$$\begin{array}{ccccccc} H_{grad} & \xrightarrow{grad} & H_{curl} & \xrightarrow{curl} & H_{div} & \xrightarrow{div} & L^2 \\ \Pi_h^0 \downarrow & & \Pi_h^1 \downarrow & & \Pi_h^2 \downarrow & & \Pi_h^3 \downarrow \\ W_h^0 & \xrightarrow{grad} & W_h^1 & \xrightarrow{curl} & W_h^2 & \xrightarrow{div} & W_h^3 \end{array}$$

that commutes, that is one can follow the arrows along any path between two spaces and obtain the same operator between these two spaces.

The construction of the generic FE subspace W_h is done according to classical steps [10], [26]. One introduces first the triple (K, P, Σ) where K is the kind of brick (triangle or tetrahedron in this case) contained in the mesh τ_h over $\bar{\Omega}$, P is a finite-dimensional vector space defined on K and Σ is a set of real-valued linear functionals σ_i , called degrees of freedom (dofs), acting on P with the property of determining uniquely any element z of P once the values $\sigma_i(z)$ are known. One then defines the FE subspace as $W_{h,r}^p = \{u \in H_{\mathcal{L}}, u|_K \in P, \forall K \in \tau_h\}$, where the integer r denotes the maximal polynomial degree of $u|_K$ (resp. of the components of $u|_K$) for scalar (resp. vector) fields $u \in H_{\mathcal{L}}$ and the integer p refers to the geometrical dimension involved to define the dofs for $u|_K$ at the lowest degree. Note that $W_{h,r}^p$ respects globally, on the whole domain, the smoothness requirements of the underlying functional space $H_{\mathcal{L}}$ associated with the boundary value problem to be approximated, and P is a suitable approximation of $H_{\mathcal{L}}$ locally, in each element K .

FE subspaces $W_{h,r}^0 \subset H_{grad}$, and $W_{h,r}^3 \subset L^2$, are well documented in the literature, sets of basis functions of arbitrary order r on tetrahedra are explicitly detailed in books [27], [17]. The vector space P consists of scalar piece-wise polynomials, chosen in such a way that the approximated function is either continuous, for $W_{h,r}^0$ (with $r \geq 1$), or discontinuous, for $W_{h,r}^3$, across the inter-element boundaries. The subspaces $W_{h,r}^0$ and $W_{h,r}^3$ are discussed in the present work for sake of completeness, as they are part of the complex.

FE subspaces $W_{h,r}^1 \subset H_{curl}$ and $W_{h,r}^2 \subset H_{div}$ exist thanks to the celebrated pioneering works described in [19] and [5], at the origin of a huge literature on the same subject. They are characterized by a space P consisting of vectors with polynomial components, chosen in such a way that the approximated field has inter-element continuity requirements (or conformity conditions) more complicated than before. The

subspace $W_{h,r}^1$ (resp. $W_{h,r}^2$) requires that the tangential (resp. normal) component of the FE approximation is continuous. These conditions are weaker than those associated with the space $W_{h,r}^0$ but their realization can be nevertheless problematic. A first difficulty at the programming level is related to the complexity of generating element basis functions for $W_{h,r}^1$ and $W_{h,r}^2$ when $r > 1$. For example, the space $W_{h,r}^1$ is spanned by vector fields with *incomplete* or *trimmed* polynomials of degree $\leq r$ as components: this means that some of the top-degree monomials are removed to satisfy some constraints. Most of the existing literature is instead about the new (second family of) FEs defined in [20]. Indeed, the definition of P is simpler, as P is now a set of vectors with *complete* polynomials of degree $\leq r$ as components (see for example [28], [1] and [13]). A second difficulty is due to the fact that dofs are not of Lagrange type. The functionals σ_i involve integrals along a curve or across a surface, with orientation to make things more complicated. For the lower degree, dofs are circulations or fluxes of the considered field, but for higher orders, when $r > 1$, dofs are *moments*, that are integrals over sub-simplices s of the vector \mathbf{z} (or of a component of it) against some test functions using some measure defined over s .

In this work, we consider the set of basis functions for the high order case recently defined in [25], [9] and show how this choice simplifies the difficulties encountered with generators and dofs for these spaces. In Section 2, we review the construction of generators for the spaces $W_{h,r}^p$, $p = 0, 1, 2, 3$, in a tetrahedron, for the lower order case, that is $r = 1$ when $p < 3$ and $r = 0$ for $p = 3$. We then face the high order case in Section 3, with the definition of small simplices and subspace generators. In Section 4 the definition of classical dofs by moments is presented and revisited in terms of the new generators. How to re-establish duality between dofs and generators is commented in Section 5. This section ends with a number of Examples that detail dofs, generators and the duality coefficients, for fields in $W_{h,r}^p$ for some values of p , r and the ambient space dimension d , providing a useful indication in view of the implementation. Numerical evidence on a classical problem of the properties for the considered generators for high order edge element spaces $W_{h,r}^1$ is given in Section 6 and some concluding remarks are set in Section 7.

2 FE subspaces $W_{h,r}^p$ for the lower polynomial order

In this section, some notations are introduced together with basic concepts about interpolating scalar and vector fields on simplicial meshes.

Let $\Omega \subset \mathbb{R}^3$ be a bounded domain with piecewise smooth boundary Γ . We consider a simplicial mesh of $\bar{\Omega}$, that is a tessellation of $\bar{\Omega}$ by tetrahedra, subject to the condition that any two of them may intersect along a common face, edge or node, but in no other way. We denote by \mathcal{N} , \mathcal{E} , \mathcal{F} , \mathcal{T} (resp. N, E, F, T) the sets (resp. the cardinality of the sets) of simplices of dimension 0 to 3 (nodes, edges, faces, and tetrahedra,

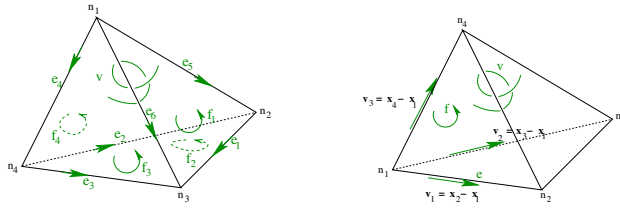


Fig. 1 The oriented tetrahedron $v = \{n_1, n_2, n_3, n_4\}$ with oriented p -faces, $0 < p < 3$ (left). The boundary of the face $f_1 = \{n_1, n_3, n_2\}$ is $\partial(f_1) = -e_1 - e_5 + e_6$. It can be identified with the vector $(-1, 0, 0, 0, -1, 1)$ collecting the coefficients in front of each edge, first line of the incidence matrix \mathbf{R} for v . The (inner) orientation of entities based on the global numbering of the vertices defining the entity (right). Here, it is assumed that the vertex n_1 with the lowest global numbering is singled out as ‘origin’ vertex for local vectors $\mathbf{v}_1, \mathbf{v}_2, \mathbf{v}_3$.

resp.) thus obtained, and by τ_h the mesh itself, with $h > 0$ standing for the maximal diameter of the tetrahedra of \mathcal{T} . Note that if a simplex s belongs to the mesh τ_h , all simplices that form the boundary of s also belong to τ_h ; each simplex appears only once in τ_h . Labels n, e, f, v are used for nodes (0-simplices), edges (1-simplices), etc. The placement of the mesh stands for the function from \mathcal{N} to $\bar{\Omega}$, giving for each node n_i its position \mathbf{x}_i in $\bar{\Omega}$. The tetrahedron $v = \{n_1, n_2, n_3, n_4\}$ is defined as the nondegenerate convex envelope of four points n_1, n_2, n_3, n_4 in \mathbb{R}^3 , where nondegenerate means $(\mathbf{x}_2 - \mathbf{x}_1) \times (\mathbf{x}_3 - \mathbf{x}_1) \cdot (\mathbf{x}_4 - \mathbf{x}_1)$ different from zero, with \mathbf{x}_i the position of n_i in \mathbb{R}^3 . Similarly, a p -simplex s , $0 \leq p \leq 3$, is the nondegenerate convex envelope of $p + 1$ geometrically distinct points n_1, \dots, n_{p+1} . The points n_1, \dots, n_{p+1} are called vertices of s , and p is the dimension of the p -simplex s , which we shall denote $s = \{n_1, \dots, n_{p+1}\}$. Any $(p - 1)$ -simplex that is a subset of $\{n_1, \dots, n_{p+1}\}$ is called $(p - 1)$ -face of s .

Besides the list of nodes and of their positions, the mesh data structure also contains incidence matrices, saying which node belongs to which edge, which edge bounds which face, etc., and there is a notion of (inner) orientation of the simplices to consider. In short, an edge, face, etc., is not only a two-node, three-node, etc., subset of \mathcal{N} , but such a set plus an orientation of the simplex it subtends. For example, $e = \{n_i, n_j\}$, where we assume that $n_i < n_j$ for simplicity at the implementation step, denotes the edge that connects the global vertices n_i and n_j , oriented in such a way that the tangent vector goes from the vertex n_i to the vertex n_j . If $e = \{n_i, n_j\}$, the edge $\{n_j, n_i\}$ is referred to as $-e$. One introduces the so-called incidence numbers $\partial_{e, n_i} = -1$, $\partial_{e, n_j} = 1$, and $\partial_{e, n_k} = 0$ for nodes n_k other than n_i and n_j . They form a rectangular matrix $\mathbf{G} = (\partial_{e, n})$, with E rows and N columns, which describes how edges connect to nodes. Faces are also oriented, not merely a collection of 3 nodes. For example, $f = \{n_i, n_j, n_k\}$, where we assume that $n_i < n_j < n_k$ for simplicity, is the face with the three vertices n_i, n_j, n_k , oriented such that the vectors $\mathbf{x}_j - \mathbf{x}_i, \mathbf{x}_k - \mathbf{x}_i$, form a reference frame in the plane supporting f . An (inner) orientation of f induces an orientation of its boundary and, with respect to this induced orientation, an edge runs

along or not. One introduces the incidence number $\boldsymbol{\partial}_{f,e}$, as +1 if e runs along the boundary of f , -1 otherwise, and 0 if e is not one of the edges of f . They form a rectangular matrix $\mathbf{R} = (\boldsymbol{\partial}_{f,e})$, with F rows and E columns. A matrix $\mathbf{D} = (\boldsymbol{\partial}_{v,f})$, indexed over \mathcal{T} and \mathcal{F} , is similarly defined: $\boldsymbol{\partial}_{v,f} = \pm 1$ if face f bounds tetrahedron v , the sign depending on whether the orientations of f and of the boundary of v match or not. This makes sense only after the tetrahedron v itself has been oriented, and the convention will be that if $v = \{n_i, n_j, n_k, n_l\}$, the vectors $\mathbf{x}_j - \mathbf{x}_i$, $\mathbf{x}_k - \mathbf{x}_i$, and $\mathbf{x}_l - \mathbf{x}_i$, in this order, define a positive frame. So, the incidence number $\boldsymbol{\partial}_{v,f} = 1$ (resp. -1) if the normal of the oriented face f is outward (resp. inward). Implicitly, we have been orienting all nodes the same way, (+1) up to now. By looking at Fig. 1, the three incidence matrices are

$$\mathbf{G} = \begin{pmatrix} 0 & -1 & 1 & 0 \\ 0 & 1 & 0 & -1 \\ 0 & 0 & 1 & -1 \\ -1 & 0 & 0 & 1 \\ -1 & 1 & 0 & 0 \\ -1 & 0 & 1 & 0 \end{pmatrix}, \quad \mathbf{R} = \begin{pmatrix} -1 & 0 & 0 & 0 & -1 & 1 \\ -1 & -1 & 1 & 0 & 0 & 0 \\ 0 & 0 & 1 & 1 & 0 & -1 \\ 0 & 1 & 0 & 1 & -1 & 0 \end{pmatrix}, \quad \mathbf{D} = (1 \ -1 \ 1 \ -1).$$

The well-known property of incidence matrices is here recalled.

Proposition 1 $\mathbf{DR} = \mathbf{0}$ and $\mathbf{RG} = \mathbf{0}$.

Proof Let $e \in \mathcal{E}$ and $v \in \mathcal{T}$. Then, by definition of matrix product, $(\mathbf{DR})_{v,e} = \sum_{f \in \mathcal{F}} \boldsymbol{\partial}_{v,f} \boldsymbol{\partial}_{f,e}$. The only nonzero terms are for faces f that both contain the edge e and bound the volume v , which means that e is an edge of v . There are exactly two faces f and g of v sharing the edge e . If $\boldsymbol{\partial}_{v,g} = \boldsymbol{\partial}_{v,f}$, then their boundaries are oriented in such a way that e must run along one and counter the other, so $\boldsymbol{\partial}_{g,e} = -\boldsymbol{\partial}_{f,e}$, and the sum is zero. If $\boldsymbol{\partial}_{v,g} = -\boldsymbol{\partial}_{v,f}$, the opposite happens, that is $\boldsymbol{\partial}_{g,e} = \boldsymbol{\partial}_{f,e}$, with the same final result. The proof of $\mathbf{RG} = \mathbf{0}$ is similar.

To make more compact the layout of a formula, the node $n = n_l$ can be denoted as $e - n$ when $e = \{n_i, n_l\}$. The same node becomes $f - e$ when $e = \{n_i, n_j\}$ and $f = \{n_i, n_j, n_l\}$ or $v - f$ when $v = \{n_i, n_j, n_l, n_q\}$ and $f = \{n_i, n_j, n_q\}$.

We now assign a function or a vector field to all simplices of the mesh. For each node $n \in \mathcal{N}$, we denote by D_n the cluster of tetrahedra in \mathcal{T} which have a vertex at n . With the node $n \in \mathcal{N}$, we associate the continuous, piecewise affine function w^n defined as

$$w^n(\mathbf{x}) = \begin{cases} \lambda_n(\mathbf{x}), & \mathbf{x} \in \bar{D}_n, \\ 0, & \text{otherwise,} \end{cases}$$

where $\lambda_n(\mathbf{x})$ is the barycentric or volume coordinate of \mathbf{x} with respect to n computed in the tetrahedron of D_n containing \mathbf{x} . By construction, \bar{D}_n coincides with the support of w^n and $\sum_{n \in \mathcal{N}} w^n(\mathbf{x}) = 1$, for all $\mathbf{x} \in \bar{D}_n$. Let us denote $\mathbb{P}_1(v)$ the vector space

of first order polynomials defined in v : it is generated by the functions w^n , with n a vertex of v . One has the *nodal* FE (K, P, Σ) for the approximation of scalar fields in v with $K = v$, $P = \mathbb{P}_1(v)$, $\Sigma = \{\sigma_n : z \mapsto z(\mathbf{x}_n), n \text{ a vertex of } v\}$. Then, $W_{h,1}^0 = \text{span}\{w^n, n \in \mathcal{N}\}$ and its functions are continuous over $\bar{\Omega}$. The interpolation operator $\Pi_h^0 : Y^0 \subset H_{grad} \rightarrow W_{h,1}^0$ associates a function $z \in Y^0$ with its decomposition on the w^n defined as $\Pi_h^0 z(\mathbf{x}) = \sum_{n \in \mathcal{N}} \sigma_n(z) w^n(\mathbf{x})$, for all $\mathbf{x} \in \bar{\Omega}$.

Next, with the edge $e = \{n_i, n_j\}$, one associates the vector field

$$\mathbf{w}^e = \lambda_{n_i} \nabla \lambda_{n_j} - \lambda_{n_j} \nabla \lambda_{n_i}.$$

It can be shown (see, *e.g.*, Proposition 2 in [8]) that the \mathbf{w}^e , varying e among the edges of v , generate the vector space $R(v) = \{\mathbf{w} \in \mathbb{R}^3, \mathbf{w}(\mathbf{x}) = \mathbf{a} \times \mathbf{x} + \mathbf{b}, \mathbf{a}, \mathbf{b} \in \mathbb{R}^3\}$. One has the *edge* FE (K, P, Σ) for the approximation of vector fields in v with $K = v$, $P = R(v)$, $\Sigma = \{\sigma_e : \mathbf{z} \mapsto \frac{1}{|e|} \int_e \mathbf{z} \cdot \mathbf{t}_e, e \text{ an edge of } v\}$, where $\mathbf{t}_e = \mathbf{x}_j - \mathbf{x}_i$ for $e = \{n_i, n_j\}$. One has $W_{h,1}^1 = \text{span}\{\mathbf{w}^e, e \in \mathcal{E}\}$ and its vectors have tangential component continuous across the inter-element faces. The interpolation operator $\Pi_h^1 : Y^1 \subset H_{curl}(\Omega) \rightarrow W_{h,1}^1$ assigns to a vector $\mathbf{z} \in Y^1$ its decomposition on the \mathbf{w}^e , defined as $\Pi_h^1 \mathbf{z}(\mathbf{x}) = \sum_{e \in \mathcal{E}} \sigma_e(\mathbf{z}) \mathbf{w}^e(\mathbf{x})$, for all $\mathbf{x} \in \bar{\Omega}$.

Similarly, with the face $f = \{n_i, n_j, n_k\}$, one associates the vector field

$$\mathbf{w}^f = 2(\lambda_{n_i} \nabla \lambda_{n_j} \times \nabla \lambda_{n_k} + \lambda_{n_j} \nabla \lambda_{n_k} \times \nabla \lambda_{n_i} + \lambda_{n_k} \nabla \lambda_{n_i} \times \nabla \lambda_{n_j}).$$

It can be shown (see [8], Proposition 2) that the \mathbf{w}^f , varying f among the faces of v , generate the vector space $D(v) = \{\mathbf{w} \in \mathbb{R}^3, \mathbf{w}(\mathbf{x}) = \mathbf{a} + b\mathbf{x}, \mathbf{a} \in \mathbb{R}^3, b \in \mathbb{R}\}$. One has the *face* FE (K, P, Σ) for the approximation of vector fields in v with $K = v$, $P = D(v)$, $\Sigma = \{\sigma_f : \mathbf{z} \mapsto \frac{1}{|f|} \int_f \mathbf{z} \cdot \mathbf{n}_f, f \text{ a face of } v\}$, where $\mathbf{n}_f = (\mathbf{x}_j - \mathbf{x}_i) \times (\mathbf{x}_k - \mathbf{x}_i)/2$ for $f = \{n_i, n_j, n_k\}$. One has $W_{h,1}^2 = \text{span}\{\mathbf{w}^f, f \in \mathcal{F}\}$ and its vectors have normal component continuous across the inter-element faces. The interpolation operator $\Pi_h^2 : Y^2 \subset H_{div}(\Omega) \rightarrow W_{h,1}^2$ associates a vector $\mathbf{z} \in Y^2$ with its decomposition on the \mathbf{w}^f defined as $\Pi_h^2 \mathbf{z}(\mathbf{x}) = \sum_{f \in \mathcal{F}} \sigma_f(\mathbf{z}) \mathbf{w}^f(\mathbf{x})$, for all $\mathbf{x} \in \bar{\Omega}$. For suitable spaces Y^p , $p = 0, 1, 2$ and $d = 3$, see [12].

Last, with the volume v , one associates the scalar field defined as

$$w^v(\mathbf{x}) = \begin{cases} \frac{1}{|v|}, & \mathbf{x} \in v, \\ 0, & \text{otherwise,} \end{cases}$$

where $|v| = \int_v 1$. One has the *volume* FE (K, P, Σ) for the approximation of scalar fields in v with $K = v$, $P = \mathbb{P}_0(v)$, $\Sigma = \{\sigma_v : z \mapsto \int_v z\}$. Then, $W_{h,0}^3 = \text{span}\{w^v, v \in \mathcal{T}\}$ and its functions are discontinuous across the inter-element faces. The interpolation operator $\Pi_h^3 : L^2(\Omega) \rightarrow W_{h,0}^3$ associates a function $z \in L^2(\Omega)$ with its decomposition on the w^v defined as $\Pi_h^3 z(\mathbf{x}) = \sum_{v \in \mathcal{T}} \sigma_v(z) w^v(\mathbf{x})$, for all $\mathbf{x} \in \bar{\Omega}$.

As pointed out in [6], the generators of FE subspace $W_{h,r}^p$, $p = 0, 1, 2, 3$, correspond to constructs in algebraic topology known as Whitney forms [30] (see [8] for a short

presentation). The key aspect of Whitney forms is that they are, at the same time, a tool to describe manifolds of dimension p by p -chains (formal weighted sum of geometrical objects of dimension p) and fields defined on these manifolds by p -cochains (applications which assign a real number to p -chains). The geometrical approach together with all associated notions (manifolds/chains and their operators, forms/cochains and their operators, ...) yields an explicit expression of the basis vectors for the vector space P and makes it possible to fully understand why the expression of these vectors is that one and not another. The following recursive definition of Whitney p -forms in a simplex v of lower degree has been firstly stated in [7].

Definition 1 For $p = 0$, we set $w^n = \lambda_n$, for all 0-simplices $n \in \mathcal{N}$. For any integer $0 < p \leq 3$, where 3 is the ambient dimension in Ω , the *Whitney p -form* w^s associated with the p -simplex s of a mesh τ_h in $\bar{\Omega}$ is

$$w^s = \sum_{\sigma \in \{(p-1)\text{-simplices}\}} \partial_{s,\sigma} \lambda_{s-\sigma} dw^\sigma \quad (1)$$

where $\partial_{s,\sigma}$ is the incidence matrix entry linking σ to s , w^σ is the $(p-1)$ -form associated with σ , and d is the exterior derivative operator from $(p-1)$ -forms to p -forms (which is related to the boundary operator ∂ from p -chains to $(p-1)$ -chains by the Stokes theorem¹: $\int_S dw = \int_{\partial S} w$, for all p -chains S and $(p-1)$ -forms w).

The expression of the scalar and vector generators for the FE spaces introduced so far can be recovered starting from Definition 1. For $W_{h,1}^1(v)$ it is sufficient to replace the exterior derivative operator d by the gradient operator ∇ . So, for the edge $e = \{l, m\}$, the identity $w^e = \sum_{n \in \mathcal{N}} \partial_{e,n} \lambda_{e-n} dw^n$ gives $w^e = \lambda_l dw^m - \lambda_m dw^l$, thus the vector function $\mathbf{w}^e = \lambda_l \nabla \lambda_m - \lambda_m \nabla \lambda_l$. For functions in $W_{h,1}^2(v)$ and $W_{h,0}^3(v)$, some additional properties are necessary, namely:

- (i) $d \circ d = 0$ (related to the fact that $\partial \circ \partial = 0$);
- (ii) $d(\alpha w) = d\alpha \wedge w + \alpha dw$, being α a scalar field, w a form and \wedge the exterior product between forms (see [3] for more details);
- (iii) ${}^1u \wedge {}^1z = {}^2(u \times z)$, where 1u denotes a 1-form, 2u a 2-form and \times is the cross product between ordinary vectors.

For $W_{h,1}^2(v)$, let us consider the tetrahedron $v = \{k, l, m, n\}$ and its face $f = \{l, m, n\}$. For all the oriented edges e of v that do not constitute the boundary of f , the quantities $\partial_{f,e}$ are 0 whereas for $e = \{l, m\}$ or $\{m, n\}$ or $\{n, l\}$ we have $\partial_{f,e} = 1$. In this case, $w^f = \sum_{e \in \mathcal{E}} \partial_{f,e} \lambda_{f-e} dw^e$ yields $w^f = \lambda_n d(\lambda_l dw^m - \lambda_m dw^l) + \lambda_l d(\lambda_m dw^n - \lambda_n dw^m) +$

¹ For $u \in H_{grad}(\Omega)$, Stokes theorem reads: $\int_\Gamma (\nabla u) \cdot \mathbf{t}_\Gamma = u(\mathbf{x}_{n_{e_\Gamma}}) - u(\mathbf{x}_{n_{s_\Gamma}})$, for any oriented curve $\Gamma \subset \Omega$ starting at $\mathbf{x}_{n_{s_\Gamma}}$, ending at $\mathbf{x}_{n_{e_\Gamma}}$, with unit tangent vector \mathbf{t}_Γ . For $\mathbf{u} \in H_{curl}(\Omega)$, Stokes theorem reads: $\int_S (\nabla \times \mathbf{u}) \cdot \mathbf{n}_S = \int_{\partial S} \mathbf{u} \cdot \mathbf{t}_{\partial S}$, for any oriented surface $S \subset \Omega$ of boundary ∂S , with outer unit normal \mathbf{n}_S and unit tangent vector $\mathbf{t}_{\partial S}$. For $\mathbf{u} \in H_{div}(\Omega)$, Stokes theorem reads: $\int_V \nabla \cdot \mathbf{u} = \int_{\partial V} \mathbf{u} \cdot \mathbf{n}_{\partial V}$, for any oriented volume $V \subset \Omega$ of boundary ∂V , with outer unit normal $\mathbf{n}_{\partial V}$.

$\lambda_m d(\lambda_n dw^l - \lambda_l dw^n)$. Then, using (i) and (ii), we get, for instance, $d(\lambda_l dw^m) = \lambda_l ddw^m + d\lambda_l \wedge dw^m = d\lambda_l \wedge d\lambda_m$ (being $w^m = \lambda_m$). We thus obtain $w^f = 2(\lambda_n d\lambda_l \wedge d\lambda_m + \lambda_l d\lambda_m \wedge d\lambda_n + \lambda_m d\lambda_n \wedge d\lambda_l)$. Finally, using (iii) and replacing d by ∇ , we get $\mathbf{w}^f = 2(\lambda_n \nabla \lambda_l \times \nabla \lambda_m + \lambda_l \nabla \lambda_m \times \nabla \lambda_n + \lambda_m \nabla \lambda_n \times \nabla \lambda_l)$, i.e., the vector function associated with f . For $W_{h,0}^3(v)$, one gets $w^v = 1/|v|$.

On the basis of the recursive formula, it is easy to see that

$$\text{grad}(W_{h,1}^0) \subset W_{h,1}^1, \quad \text{curl}(W_{h,1}^1) \subset W_{h,1}^2, \quad \text{div}(W_{h,1}^2) \subset W_{h,0}^3.$$

It can also be shown that the value of w^n is equal to 1 at \mathbf{x}_n and 0 at \mathbf{x}_m for all $m \in \mathcal{N}$, $m \neq n$, the circulation of \mathbf{w}^e along the edge e is 1 and 0 along $e' \in \mathcal{E}$, $e' \neq e$, the flux of \mathbf{w}^f across the face f is 1 and 0 across $f' \in \mathcal{F}$, $f' \neq f$, the integral of w^v over the tetrahedron v is 1 and 0 over $v' \in \mathcal{T}$, $v' \neq v$. This means that the basis functions are in duality with the selected dofs. Another way to state the property of duality is by introducing the matrices of weights, that are square matrices \mathbf{V}^p , one for each value of $p = 0, 1, 2, 3$, with entries defined as

$$\begin{aligned} (\mathbf{V}^0)_{ij} &= w^{n_j}(\mathbf{x}_i), & n_i, n_j \in \mathcal{N}, \quad i, j \in \{1, \dots, \mathbf{N}\}, \\ (\mathbf{V}^1)_{ij} &= \frac{1}{|e_i|} \int_{e_i} \mathbf{w}^{e_j} \cdot \mathbf{t}_{e_i}, & e_i, e_j \in \mathcal{E}, \quad i, j \in \{1, \dots, \mathbf{E}\}, \\ (\mathbf{V}^2)_{ij} &= \frac{1}{|f_i|} \int_{f_i} \mathbf{w}^{f_j} \cdot \mathbf{n}_{f_i}, & f_i, f_j \in \mathcal{F}, \quad i, j \in \{1, \dots, \mathbf{F}\}, \\ (\mathbf{V}^3)_{ij} &= \int_{v_i} w^{v_j}, & v_i, v_j \in \mathcal{T}, \quad i, j \in \{1, \dots, \mathbf{T}\}. \end{aligned}$$

When duality holds for a value of p , the corresponding matrix of weights is the identity. As a consequence of duality and Stokes theorem, if one sets, for example, $\mathbf{z} = \nabla \varphi$, where $\varphi = \sum_{n \in \mathcal{N}} \varphi(\mathbf{x}_n) w^n$ is an element of $W_{h,1}^0$, then $\mathbf{z} \in W_{h,1}^1$ is expressed as $\sum_{e \in \mathcal{E}} z_e \mathbf{w}^e$, with $z_e = \varphi(\mathbf{x}_j) - \varphi(\mathbf{x}_i)$ if $e = \{n_i, n_j\}$. Now, let (z_e) be the vector of length \mathbf{E} collecting the circulations z_e of \mathbf{z} along the edges $e \in \mathcal{E}$, and (φ_n) the vector of length \mathbf{N} collecting the values $\varphi(\mathbf{x}_n)$ of φ at the nodes $n \in \mathcal{N}$. Then, $(z_e) = \mathbf{G}(\varphi_n)$ where \mathbf{G} is the edge-to-node incidence matrix, which thus appears as a discrete analogue of the gradient operator. Similarly, the face-to-edge (resp. volume-to-face) incidence matrix \mathbf{R} (resp. \mathbf{D}) appears as a discrete analogue of the curl (resp. divergence) operator. Note that duality is generally lost when we move to higher order. In the following, we show that, with the high order generators defined in [25] and field moments as dofs, in the style of those presented in [19], the generator/dof duality is easy to restore.

3 The small p -simplices and Whitney forms of higher degree

Definitions of higher order Whitney forms, that is for $r > 1$, were firstly presented in [15], [16], and more recently in [3]. An explicit expression for edge FE basis vectors on simplices in terms of affine coordinates has been given in [14]. Despite this, the application of the higher order Whitney forms has not spread out. This makes think that the expression of these forms is not easy to handle.

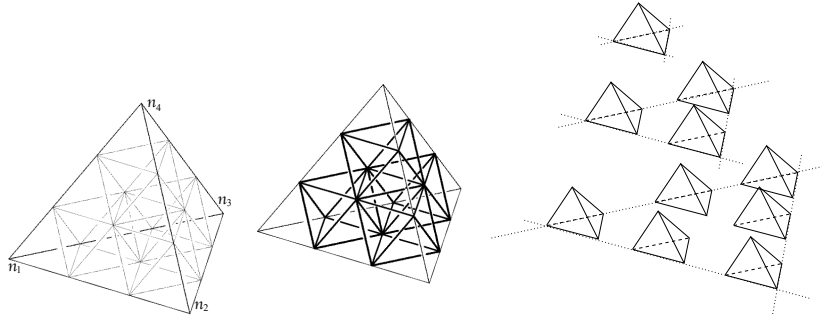


Fig. 2 For $d = 3$ and $r = 3$, the edges connecting the points of $T_3(v)$ (left), the holes in thick line (center), the small d -simplices in the exploded configuration (right). The small 0-simplices are nothing else than the nodes of $T_3(v)$. Starting from the nodes of $T_3(v)$, we may construct 60 small edges, 40 small faces, 10 small tetrahedra.

Adopting a geometrical approach to define higher order Whitney forms we have to construct a finer description of p -chains in the volume v , $0 \leq p \leq d$, where d is the ambient space dimension. This procedure is classically used to define higher order nodal FEs for scalar fields [10]: it goes through the introduction of the principal lattice of order $r \geq 1$ in the volume $v \subset \mathbb{R}^d$. It consists in the set of points

$$T_r(v) = \left\{ \mathbf{x} \in v, \lambda_j(\mathbf{x}) \in \left\{ 0, \frac{1}{r}, \frac{2}{r}, \dots, \frac{(r-1)}{r}, 1 \right\}, 1 \leq j \leq d+1 \right\}.$$

We recall that (the proof is by recurrence on d) the cardinality of $T_r(v)$ is equal to the dimension of $\mathbb{P}_r(v)$, the space of real-valued polynomials defined in \mathbb{R}^d , restricted to the volume v , of degree $\leq r$. The functionals $\sigma_l : z \mapsto z(\mathbf{x}_l)$, with $\mathbf{x}_l \in T_r(v)$, are classically taken as dofs for functions in $\mathbb{P}_r(v)$.

Here, since we deal also with fields whose physical meaning is specified by circulations along curves or fluxes across surfaces or densities in volumes, we need to define dofs accordingly, even when we consider a high order approximation of those fields. We have thus to create a sort of principal lattice of edges, faces and volumes in v for $r > 1$. This is realized by connecting the points of $T_r(v)$ with planes parallel to the faces of v , (as in Fig. 2, left). One thus obtains a partition of v including d -simplices homothetic to v (the so-called “small” d -simplices, visible in Fig. 2 right) and other objects (the “holes”, the objects with thick boundary in Fig. 2, center) that can only be octahedra and reversed tetrahedra when v is a tetrahedron. Any p -simplex, $0 \leq p < d$, belonging to the boundary of a small d -simplex is called small p -simplex.

To formalize the construction defined right above, we need to introduce multi-index notations. Let \mathbf{k} , boldface, be the array (k_1, \dots, k_{d+1}) of $d+1$ integers $k_i \geq 0$, and denote by k its weight $\sum_{i=1}^{d+1} k_i$. The set of multi-indices \mathbf{k} with $d+1$ components and of weight k is denoted $\mathcal{I}(d+1, k)$. We may now state the following definition.

Definition 2 Let us consider the principal lattice $T_r(v)$ of order $r > 1$ in the simplex $v = \{n_1, \dots, n_{d+1}\}$. The *small simplex* $\{\mathbf{k}, s\}$, with $\mathbf{k} \in \mathcal{I}(d+1, r-1)$, is a p -simplex

parallel and $1/r$ -homothetic to the (big) p -face s of v , with vertices in $T_r(v)$. It belongs to the boundary of (if $0 \leq p < d$) or coincides with (if $p = d$) the small tetrahedron whose barycenter \mathbf{g} has barycentric coordinates

$$\lambda_{n_j}(\mathbf{g}) = \frac{\left(\frac{1}{d+1} + k_j\right)}{k+1}, \quad 1 \leq j \leq d+1.$$

The barycenters of the small tetrahedra for a degree $r > 1$ are used to localize the small p -simplices. As an example, referring to Fig. 2, left and right, where $v = \{n_1, n_2, n_3, n_4\}$, one has:

- the small simplex $\{(1, 1, 0, 0), v\}$ is the *small tetrahedron* (it has the same dimension as the simplex in the curled brackets, here v) in the bottom layer, middle position and touching the edge $\{n_1, n_2\}$. Indeed, for the vector $(1, 1, 0, 0)^t$ the barycenter \mathbf{g} of this small tetrahedron verifies

$$\lambda_{n_1}(\mathbf{g}) = \frac{1}{12} + \frac{1}{3}, \quad \lambda_{n_2}(\mathbf{g}) = \frac{1}{12} + \frac{1}{3}, \quad \lambda_{n_3}(\mathbf{g}) = \frac{1}{12}, \quad \lambda_{n_4}(\mathbf{g}) = \frac{1}{12};$$

- the small simplex $\{(0, 1, 0, 1), f = \{n_1, n_2, n_4\}\}$ is the *small face* parallel to f belonging to the small tetrahedron in the middle layer, touching the edge $\{n_2, n_4\}$.

The barycenter \mathbf{g} of this latter small tetrahedron verifies

$$\lambda_{n_1}(\mathbf{g}) = \frac{1}{12}, \quad \lambda_{n_2}(\mathbf{g}) = \frac{1}{12} + \frac{1}{3}, \quad \lambda_{n_3}(\mathbf{g}) = \frac{1}{12}, \quad \lambda_{n_4}(\mathbf{g}) = \frac{1}{12} + \frac{1}{3};$$

- the small simplex $\{(0, 0, 2, 0), e = \{n_3, n_4\}\}$ is the *small edge* parallel to e belonging to the small tetrahedron in the bottom layer, corner position and touching the edge $\{n_3, n_4\}$. The barycenter \mathbf{g} of this latter small tetrahedron verifies

$$\lambda_{n_1}(\mathbf{g}) = \frac{1}{12}, \quad \lambda_{n_2}(\mathbf{g}) = \frac{1}{12}, \quad \lambda_{n_3}(\mathbf{g}) = \frac{1}{12} + \frac{2}{3}, \quad \lambda_{n_4}(\mathbf{g}) = \frac{1}{12}.$$

The complex of small simplices is not created in the reality, it is drawn to help to visualize the high order construction. In the following, we adopt the

Definition 3 Given $\mathbf{k} \in \mathcal{I}(d+1, k)$, we set $\lambda^{\mathbf{k}} = \prod_{i=1}^{d+1} (\lambda_{n_i})^{k_i}$.

Homogeneous polynomials of degree k in barycentric coordinates are in one-to-one correspondence with polynomials of degree $\leq k$ in Cartesian coordinates. For this reason, we can say that $\mathbb{P}_k(v) = \text{span}(\lambda^{\mathbf{k}})_{\mathbf{k} \in \mathcal{I}(d+1, k)}$ on each volume v . We recall that $\dim(\mathbb{P}_k(v)) = \binom{k+d}{d}$. It will occur, when revisiting dofs for scalar and vector fields, that we adopt a ‘‘simplification’’ of Definition 3, as detailed here below. Let $s = \{n_1, \dots, n_{p'+1}\}$ be a p' -simplex, $0 \leq p' \leq d$, and let $\mathbf{k}_s \in \mathcal{I}(p'+1, k')$ be a multi-index of weight k' . We thus introduce the notation

$$\lambda_s^{\mathbf{k}_s} = \prod_{i=1}^{p'+1} (\lambda_{n_i})^{(\mathbf{k}_s)_i}. \quad (2)$$

For the same reason as before, we can say that $\mathbb{P}_{k'}(s) = \text{span}(\lambda_s^{\mathbf{k}_s})_{\mathbf{k}_s \in \mathcal{I}(p'+1, k')}$ on each p' -simplex s . Finally, the definition of possible generators for $W_{h,r}^p(v)$ in a tetrahedron v is the one firstly introduced in [25], that we recall here below.

Definition 4 *Whitney p -forms of high order $r = k + 1$ for $0 \leq p \leq 2$, $r = k$ for $p = 3$ (where $k \geq 0$) in a volume v are the $\lambda^{\mathbf{k}} w^s$, for all pairs $\{\mathbf{k}, s\}$, with $\mathbf{k} \in \mathcal{I}(d + 1, k)$ and s a p -simplex. The w^s are the Whitney p -forms on s of polynomial degree 1 for $0 \leq p \leq 2$, and 0 for $p = 3$, as stated in Definition 1.*

The generators of $W_{h,r}^p(v)$ are indexed on the basis of the small simplices $\{\mathbf{k}, s\}$ introduced right above. Thanks to Definition 4, if one makes the list of the small simplices for given k and p , this immediately and explicitly yields the list of all generators of $W_{h,r}^p(v)$, with $r = k + 1$ for $0 \leq p \leq 2$, $r = k$ for $p = 3$. Whitney p -forms of higher polynomial degree r in v are thus easy to generate. For instance, if $0 \leq p \leq 2$, for second order spaces in v , say $W_{h,2}^p(v)$, consider all the products $\lambda_i w^s$, where $n_i \in \mathcal{N}$ and $w^s \in W_{h,1}^p(v)$. For third order spaces in v , say $W_{h,3}^p(v)$, consider all the products $\lambda_i \lambda_j w^s$, where $n_i, n_j \in \mathcal{N}$ and $w^s \in W_{h,1}^p(v)$, etc. We may thus write that $W_{h,r}^p(v) = \mathbb{P}_{r-1}(v) \otimes W_{h,1}^p(v)$, $r \geq 1$ if $0 \leq p \leq 2$, and $W_{h,r}^p(v) = \mathbb{P}_r(v) \otimes W_{h,0}^p(v)$, $r \geq 0$ if $p = 3$. Then, in the scalar/vector formalism, one has to replace, in each product $\lambda^{\mathbf{k}} w^s$, the form w^s by its scalar/vector field, as explained in Section 2, after Definition 1. Elements in $W_{h,r}^p$ enjoy the same conformity properties as those in $W_{h,1}^p$ since they are defined as products between an element in $W_{h,1}^p$ and the continuous function $\lambda^{\mathbf{k}}$, $\mathbf{k} \in \mathcal{I}(d + 1, k)$. However, the products $\lambda^{\mathbf{k}} w^s$ generate the spaces $W_{h,r}^p$, but don't actually constitute a basis as they are not all linearly independent. This result is stated in [25], Proposition 3.5, that we recall here.

Proposition 2 *For any edge e , face f , and tetrahedron v , we have, respectively,*

$$\sum_{n \in \mathcal{N}} \partial_{e,n} \lambda_{e-n} w^n = 0, \quad \sum_{e \in \mathcal{E}} \partial_{f,e} \lambda_{f-e} w^e = 0, \quad \sum_{f \in \mathcal{F}} \partial_{v,f} \lambda_{v-f} w^f = 0. \quad (3)$$

Proof For the edge $e = \{n_i, n_j\}$, we have $(\partial_{e,n_i}) = -1$, $(\partial_{e,n_j}) = 1$ and 0 otherwise. Therefore, we get $-\lambda_{n_j} \lambda_{n_i} + \lambda_{n_i} \lambda_{n_j} = 0$, for the definition of w^n . To prove the second identity, we replace w^e by its expression given in (1) and we get $\sum_e \partial_{f,e} \lambda_{f-e} w^e = \sum_{n,e} \lambda_{f-e} \lambda_{e-n} \partial_{f,e} \partial_{e,n} dw^n = 0$ since $(\partial_{f,e})(\partial_{e,n}) = \mathbf{0}$ and, for a fixed n vertex of f , $\lambda_{f-e} \lambda_{e-n}$ is the same for all e in ∂f . The third identity can be proved similarly, thanks to the fact that $(\partial_{v,f})(\partial_{f,e}) = \mathbf{0}$.

Due to relations (3), there exists a combination with nonzero coefficients of the forms $\lambda^{\mathbf{k}} w^s$, with $\mathbf{k} \in \mathcal{I}(d + 1, 1)$ and s a p -simplex being $0 \leq p < 3$, that gives zero. Iterating on the weight k of the multi-index \mathbf{k} , we have the linear dependency of the high order generators. Thanks to Proposition 2, one knows which are the redundant generators. Moreover, these can be easily eliminated from the list of the generators to come up with a basis for $W_{h,r}^p$ as explained in the Examples presented in Section 5.

We now have a look at possible dofs for fields in $W_{h,r}^p$. Different sets of unisolvent dofs exist for high order elements: in [24,25] we have analyzed those associated with the small-simplices. Here, we analyze separately for each value of $0 \leq p \leq 3$, and in a vector formalism, the ones referred to as moments (see Def. 6 and 7 in [19] for $p = 1, 2$).

4 High order moments for fields in $W_{h,r}^p(v)$

We start with a scalar function $z \in W_{h,r}^0(v)$, for $r \geq 1$. Instead of the classical dofs, namely the functionals $\sigma_l : z \mapsto z(\mathbf{x}_l)$, with \mathbf{x}_l a node of $T_r(v)$, we adopt new dofs, as suggested in [18]. This definition is more appropriate to see that the relevant functional spaces ($H_{grad}(v)$, $H_{curl}(v)$, $H_{div}(v)$ and $L^2(v)$) and their discrete counterparts $W_{h,r}^p(v)$ are related in the famous commutative diagram by suitable (continuous, discrete and interpolation) operators.

Definition 5 The dofs for a scalar function $z \in W_{h,r}^0(v)$, for $r \geq 1$, are the functionals

$$\sigma_n : z \mapsto z(n) \quad \forall n \in \mathcal{N} \quad (4)$$

$$\sigma_e : z \mapsto \frac{1}{|e|} \int_e z u \quad \forall u \in \mathbb{P}_{r-2}(e), \forall e \in \mathcal{E} \quad (5)$$

$$\sigma_f : z \mapsto \frac{1}{|f|} \int_f z q \quad \forall q \in \mathbb{P}_{r-3}(f), \forall f \in \mathcal{F} \quad (6)$$

$$\sigma_v : z \mapsto \frac{1}{|v|} \int_v z w \quad \forall w \in \mathbb{P}_{r-4}(v). \quad (7)$$

The first thing to remark is that in Definition 5 if $r < 4$, dofs given by (7) are not used. This is implicitly stated by the fact that it is not possible to define the elements of $\mathbb{P}_{r-4}(v)$ when $r < 4$, namely polynomials with negative degree. For the same reason, if $r < 3$, dofs given by (6) and (7) are not used. If $r < 2$, dofs given by (5), (6) and (7) are not used. Note how the polynomials given in Definition 3, together with the simplification stated in (2), make it easier the computation of dofs (5)-(7). Indeed, we may replace $u \in \mathbb{P}_{r-2}(e)$ in (5) by $\lambda_e^{\mathbf{k}_e}$ with $\mathbf{k}_e \in \mathcal{I}(p' + 1, r - 2)$, with $p' = 1$ as we are on the edge e . Similarly, we may take as $q \in \mathbb{P}_{r-3}(f)$ in (6) the polynomial $\lambda_f^{\mathbf{k}_f}$ with $\mathbf{k}_f \in \mathcal{I}(p' + 1, r - 3)$, with $p' = 2$ as we are on the face f . And for $w \in \mathbb{P}_{r-4}(v)$ we may consider the $\lambda^{\mathbf{k}}$ of Definition 3 with $\mathbf{k} \in \mathcal{I}(3 + 1, r - 4)$. We note that

$$\begin{aligned} & 4 + 6 \dim(\mathbb{P}_{r-2}(e)) + 4 \dim(\mathbb{P}_{r-3}(f)) + \dim(\mathbb{P}_{r-4}(v)) \\ &= \frac{1}{6}(r + 3)(r + 2)(r + 1) = \dim(\mathbb{P}_r(v)) \end{aligned}$$

is the total number of dofs. Dofs (4)-(7) are $W_{h,r}^0(v)$ -unisolvent, for any $r \geq 1$, as proved in [18], Section 5.6 (recall that $W_{h,r}^0(v)$ is a discrete space for $H_{grad}(v)$).

Let us move on with the well-known cases $p = 1$ and $p = 2$ that we recall in Definitions 6 and 7, respectively².

Definition 6 The dofs for a vector function $\mathbf{w} \in W_{h,r}^1(v)$, for $r \geq 1$, are the functionals

$$\sigma_e : \mathbf{w} \mapsto \frac{1}{|e|} \int_e (\mathbf{w} \cdot \mathbf{t}_e) u \quad \forall u \in \mathbb{P}_{r-1}(e), \forall e \in \mathcal{E}(v) \quad (8)$$

$$\sigma_f : \mathbf{w} \mapsto \frac{1}{|f|} \int_f (\mathbf{w} \times \mathbf{n}_f) \cdot \mathbf{q} \quad \forall \mathbf{q} \in (\mathbb{P}_{r-2}(f))^2, \forall f \in \mathcal{F}(v) \quad (9)$$

$$\sigma_v : \mathbf{w} \mapsto \frac{1}{|v|} \int_v \mathbf{w} \cdot \mathbf{z} \quad \forall \mathbf{z} \in (\mathbb{P}_{r-3}(v))^3 \quad (10)$$

with \mathbf{t}_e (resp. \mathbf{n}_f) the vector of length $|e|$ (resp. 1), tangent to e (resp. normal to f).

² Some simple formula which are involved in the definition of dofs. For the tetrahedron $v = \{n_1, n_2, n_3, n_4\}$, one has $|v| = 4 \int_v \lambda_4$; for the face $f = \{n_1, n_2, n_3\}$, one has $|f| = 3|v| |\nabla \lambda_4|$; for the edge $e = \{n_1, n_2\}$, one has $|e| = 6|v| |\nabla \lambda_3 \times \nabla \lambda_4|$, and $6|v| (\nabla \lambda_1 \times \nabla \lambda_2) \cdot \nabla \lambda_3 = 1$.

In Section 1.2 of [19] it is proved that dofs (8)-(10) are $W_{h,r}^1(v)$ -unisolvent, for any $r \geq 1$. The space $W_{h,r}^1(v)$ is indeed a discrete counterpart of $H_{curl}(v)$.

Proposition 3 *Let us consider a vector $\mathbf{w} \in W_{h,r}^1(v)$ for $r \geq 1$. Its moments on faces given by (9) are equivalent to*

$$\sigma_f : \mathbf{w} \mapsto \frac{1}{|f|} \int_f (\mathbf{w} \cdot \mathbf{t}_{f,i}) q, \quad \forall q \in \mathbb{P}_{r-2}(f), \quad \forall f \in \mathcal{F}(v),$$

$$\mathbf{t}_{f,i} \text{ two independent sides of } f, \quad i = 1, 2. \quad (11)$$

Proof Any vector $\mathbf{q} \in (\mathbb{P}_{r-2}(f))^2$ for the face $f = \{n_i, n_j, n_l\}$ (with $n_i < n_j < n_l$) can be written as a linear combination of the two independent vectors

$$\mathbf{q}_1 = \lambda_f^{\mathbf{k}_f} (\mathbf{t}_{f,1} \times \mathbf{n}_f) \quad \text{and} \quad \mathbf{q}_2 = \lambda_f^{\mathbf{k}_f} (\mathbf{t}_{f,2} \times \mathbf{n}_f) \quad (12)$$

with $\mathbf{t}_{f,1} = \mathbf{x}_j - \mathbf{x}_i$, $\mathbf{t}_{f,2} = \mathbf{x}_l - \mathbf{x}_i$ two sides defining the face f (as in Fig. 1, right), \mathbf{n}_f its normal, \mathbf{k} a multi-integer of $\mathcal{I}(3, r-2)$ and $\lambda_f^{\mathbf{k}_f}$ defined in simplification (2) of Definition 3. We use the vector identity

$$(\mathbf{a} \times \mathbf{b}) \cdot (\mathbf{c} \times \mathbf{d}) = (\mathbf{a} \cdot \mathbf{c})(\mathbf{b} \cdot \mathbf{d}) - (\mathbf{a} \cdot \mathbf{d})(\mathbf{b} \cdot \mathbf{c})$$

to see that

$$\begin{aligned} (\mathbf{w} \times \mathbf{n}_f) \cdot \mathbf{q}_1 &= (\mathbf{w} \times \mathbf{n}_f) \cdot \lambda_f^{\mathbf{k}_f} (\mathbf{t}_{f,1} \times \mathbf{n}_f) \\ &= \lambda_f^{\mathbf{k}_f} [(\mathbf{w} \cdot \mathbf{t}_{f,1})(\mathbf{n}_f \cdot \mathbf{n}_f) - (\mathbf{w} \cdot \mathbf{n}_f)(\mathbf{n}_f \cdot \mathbf{t}_{f,1})] \\ &= \lambda_f^{\mathbf{k}_f} [(\mathbf{w} \cdot \mathbf{t}_{f,1})(1) - (\mathbf{w} \cdot \mathbf{n}_f)(0)] = \lambda_f^{\mathbf{k}_f} (\mathbf{w} \cdot \mathbf{t}_{f,1}) \end{aligned}$$

and similarly with \mathbf{q}_2 . The proof ends as $\mathbb{P}_{r-2}(f) = \text{span}(\lambda_f^{\mathbf{k}_f})_{\mathbf{k} \in \mathcal{I}(3, r-2)}$.

Proposition 4 *Let us consider a vector $\mathbf{w} \in W_{h,r}^1(v)$ for $r \geq 1$. Its moments in the volume given by (10) are equivalent to*

$$\sigma_v : \mathbf{w} \mapsto \frac{1}{|v|} \int_v (\mathbf{w} \cdot \mathbf{t}_{v,i}) q, \quad \forall q \in \mathbb{P}_{r-3}(v),$$

$$\mathbf{t}_{v,i} \text{ three independent sides of } v, \quad i = 1, 2, 3. \quad (13)$$

Proof Any vector $\mathbf{q} \in (\mathbb{P}_{r-3}(v))^3$ for the volume $v = \{n_1, n_2, n_3, n_4\}$ can be written as a linear combination of the three independent vectors

$$\mathbf{q}_1 = \lambda_v^{\mathbf{k}} \mathbf{t}_{v,1}, \quad \mathbf{q}_2 = \lambda_v^{\mathbf{k}} \mathbf{t}_{v,2}, \quad \text{and} \quad \mathbf{q}_3 = \lambda_v^{\mathbf{k}} \mathbf{t}_{v,3} \quad (14)$$

where $\mathbf{t}_{v,\ell} = \mathbf{x}_{\ell+1} - \mathbf{x}_1$, for $\ell = 1, 2, 3$, \mathbf{k} a multi-integer of $\mathcal{I}(3+1, r-3)$ and $\lambda_v^{\mathbf{k}}$ defined in Definition 3. In the definition of the \mathbf{q}_i , the part $\lambda_v^{\mathbf{k}}$ allows to specify the polynomial degree $r-3$ and the polynomial variables (barycentric coordinates w.r.t. vertices of v), whereas the (constant) $\mathbf{t}_{v,\ell}$ determine the vector nature.

Definition 7 The dofs for a vector function $\mathbf{w} \in W_{h,r}^2(v)$, for $r \geq 1$, are the functionals

$$\sigma_f : \mathbf{w} \mapsto \frac{1}{|f|} \int_f (\mathbf{w} \cdot \mathbf{n}_f) q \quad \forall q \in \mathbb{P}_{r-1}(f), \forall f \in \mathcal{F}(v) \quad (15)$$

$$\sigma_v : \mathbf{w} \mapsto \frac{1}{|v|} \int_v \mathbf{w} \cdot \mathbf{z} \quad \forall \mathbf{z} \in (\mathbb{P}_{r-2}(v))^3 \quad (16)$$

with \mathbf{n}_f the vector of length $|f|$, normal to the face f .

We refer to Section 1.3 of [19] for a proof that dofs (15)-(16) are $W_{h,r}^2(v)$ -unisolvent, for any $r \geq 1$. We recall that $W_{h,r}^2(v)$ is a discrete counterpart of $H_{div}(v)$.

Proposition 5 Let us consider a vector $\mathbf{w} \in W_{h,r}^2(v)$ for $r \geq 1$. Its moments on the faces f of v given by (15) are equivalent to

$$\sigma_f : \mathbf{w} \mapsto \frac{3|v|}{|f|} \int_f (\mathbf{w} \cdot \nabla \lambda_{v-f}) q, \quad \forall q \in \mathbb{P}_{r-1}(f), \forall f \in \mathcal{F}(v). \quad (17)$$

Proof Let us assume that $f = \{n_1, n_2, n_3\}$ and $v = \{n_1, n_2, n_3, n_4\}$ (thus $v-f = \{n_4\}$), we know that $1/|\nabla \lambda_4|$ is the height of v with respect to f and that $\nabla \lambda_4$ has the same direction as \mathbf{n}_f . This yields $\mathbf{n}_f = (3|v|)\nabla \lambda_4$. Note that we may replace $q \in \mathbb{P}_{r-1}(f)$ by $\lambda_f^{\mathbf{k}_f}$ with $\mathbf{k}_f \in \mathcal{I}(p'+1, r-1)$, being $p' = 2$.

Proposition 6 Let us consider a vector $\mathbf{w} \in W_{h,r}^2(v)$ for $r \geq 1$. Its moments in the volume given by (16) are equivalent to

$$\sigma_v : \mathbf{w} \mapsto \frac{1}{|v|} \int_v (\mathbf{w} \cdot \mathbf{t}_{v,i}) q, \quad \forall q \in \mathbb{P}_{r-2}(v),$$

$$\mathbf{t}_{v,i} \text{ three independent sides of } v, i = 1, 2, 3. \quad (18)$$

Proof Same proof as the one of Proposition 4, with $q \in \mathbb{P}_{r-2}(v)$.

Definition 8 The dofs for a scalar function $w \in W_{h,r}^3(v)$, for $r \geq 0$, are

$$\sigma_v : w \mapsto \int_v wz \quad \forall z \in \mathbb{P}_r(v). \quad (19)$$

We recall that $W_{h,r}^3(v)$ is a discrete counterpart of $L^2(v)$. Here is a proof that dofs (19) are $W_{h,r}^3(v)$ -unisolvent, for any $r \geq 0$.

Proposition 7 Dofs (19) are $W_{h,r}^3(v)$ -unisolvent, for any $r \geq 0$.

Proof We recall that $W_{h,r}^3(v)$ is a finite-dimensional subspace of $L^2(v)$. Let us denote by $\{\xi_j\}_{j=1,m}$ a basis of $W_{h,r}^3(v)$, where $m = \dim(W_{h,r}^3(v))$. We define $\Sigma = \{\sigma_j, j = 1, m\}$ the set composed of the following linear forms $\sigma_j : W_{h,r}^3(v) \rightarrow \mathbb{R}$

$$\sigma_j : w \mapsto \int_v w \xi_j, \quad \forall j = 1, m.$$

These forms are the ones defined in (19): we have indeed replaced $z \in \mathbb{P}_r(v)$ by a function ξ_j , as, by construction (Definition 4, for $p = 3$) the set $\{\xi_j\}_{j=1,m}$ spans $\mathbb{P}_r(v)$.

Therefore, $\text{card}(\Sigma) = m = \dim(\mathbb{P}_r(v))$. Let $u \in W_{h,r}^3(v)$ be such that $\sigma_j(u) = 0$, for all $j = 1, m$. Writing $u = \sum_{j=1}^m c_j \xi_j$, $c_j \in \mathbb{R}$, we get

$$\int_v u^2 = \sum_{j=1}^m c_j \int_v u \xi_j = \sum_{j=1}^m c_j \sigma_j(u) = 0.$$

This yields $u = 0$ in v .

5 Restoring duality between generators and dofs

Polynomial fitting of a scalar function f at $N = r + 1$ points x_k of a real interval I in terms of the canonical basis $\{x^{i-1}\}_{i=1,\dots,N}$ of $\mathbb{P}_r(I)$ reads $f(x) \approx I_r f(x) = \sum_{i=1}^N a_i x^{i-1}$ with $f_k := f(x_k) = I_r f(x_k)$. The coefficients a_i are entries of \mathbf{a} , solution of the Vandermonde linear system $V\mathbf{a} = \mathbf{f}$ where $V_{ki} = x_k^{i-1}$. Adopting a basis $\{\psi_i\}$ for $\mathbb{P}_r(I)$ (different from the canonical one) and cardinal (or Lagrange) functions $\phi_j(x) \in \mathbb{P}_r(I)$ defined by $\phi_j(x_k) = \delta_{kj}$ to represent f , we have

$$f(x) \approx I_r(f)(x) = \sum_{j=1}^N u_j \psi_j(x) = \sum_{k=1}^N f_k \phi_k(x).$$

Combining these conditions yields the transformations

$$V\mathbf{u} = \mathbf{f} \quad \text{and} \quad \psi_j(x) = \sum_{k=1}^N V_{jk}^t \phi_k(x),$$

where V is the generalized Vandermonde matrix with entries $V_{ij} = \psi_j(x_i)$. Therefore, $\phi_k(x) = \sum_{j=1}^N c_{kj} \psi_j(x)$, where $\mathbf{c}_k = (c_{k1}, c_{k2}, \dots, c_{kN})^t$ is the k -th column of V^{-1} .

The methodology to construct cardinal functions in $W_{h,r}^p$ is the same as the one used in the scalar case. The generalized Vandermonde matrix to consider is \mathbf{V}^p , with entries $(\mathbf{V}^p)_{ij} = \sigma_i(\mathbf{w}_j)$, for $i, j = 1, m$, where $m = \dim(W_{h,r}^p)$ for a chosen $0 \leq p \leq d$ and $r \geq 1$. The $\{\mathbf{w}_j\}$ are a linearly independent subset of the generators given in Definition 4 and the σ_i are the moments for fields in $W_{h,r}^p$. With high order methods, it is usual to have dofs not in duality with the basis functions, as both sets are chosen in order to optimize some physical or computational criteria. Here, for $r > 1$, the matrix \mathbf{V}^p is non-singular but different from the identity. Duality can however be re-established by considering suitable linear combinations of the original generators. We wish to find coefficients c_{kj} that give new basis functions $\tilde{\mathbf{w}}_k = \sum_{j=1}^m c_{kj} \mathbf{w}_j$, $k = 1, m$, such that $\sigma_i(\tilde{\mathbf{w}}_j) = \delta_{ij}$. Let us consider a field $\mathbf{z} \in W_{h,r}^p(v)$, then

$$\mathbf{z} = \sum_{j=1}^m \alpha_j \mathbf{w}_j = \sum_{k=1}^m \beta_k \tilde{\mathbf{w}}_k$$

for two uniquely defined vectors $\boldsymbol{\alpha} = (\alpha_j)$, $\boldsymbol{\beta} = (\beta_k)$ in \mathbb{R}^m . By linearity, we obtain

$$\sum_{j=1}^m \alpha_j \sigma_i(\mathbf{w}_j) = \sum_{k=1}^m \beta_k \sigma_i(\tilde{\mathbf{w}}_k) = \beta_i, \quad \forall i = 1, m,$$

that is $\mathbf{V}^p \boldsymbol{\alpha} = \boldsymbol{\beta}$. The identity $\beta_k = \sum_{j=1}^m \mathbf{V}_{kj}^p \alpha_j$ yields

$$\sum_{j=1}^m \alpha_j \mathbf{w}_j = \sum_{k=1}^m \left(\sum_{j=1}^m \mathbf{V}_{kj}^p \alpha_j \right) \tilde{\mathbf{w}}_k = \sum_{j=1}^m \alpha_j \left(\sum_{k=1}^m \mathbf{V}_{kj}^p \tilde{\mathbf{w}}_k \right).$$

By identification, we have that

$$\mathbf{w}_j = \sum_{k=1}^m \mathbf{V}_{kj}^p \tilde{\mathbf{w}}_k = \sum_{k=1}^m (\mathbf{V}^p)_{jk}^t \tilde{\mathbf{w}}_k.$$

It thus results that the coefficients c_{kj} to express the new basis functions $\tilde{\mathbf{w}}_k$ as a linear combination of the generators \mathbf{w}_j are the entries of the k -th column of $(\mathbf{V}^p)^{-1}$.

The interpolation operator $\Pi_{h,r}^p$ from, respectively, $Y^0 \subset H_{grad}(v)$ for $p = 0$, $Y^1 \subset H_{curl}(v)$ for $p = 1$, $Y^2 \subset H_{div}(v)$ for $p = 2$ and $L^2(v)$ for $p = 3$, to $W_{h,r}^p$ reads $\Pi_{h,r}^p z(\mathbf{x}) = \sum_{i=1}^m c_i \tilde{w}_i(\mathbf{x})$, with z and \tilde{w}_i being scalar or vector functions, accordingly. Thanks to duality, the unknown coefficient c_i associated with the i -th basis function \tilde{w}_i is exactly the value $\sigma_i(z)$, resulting from the application of σ_i on z . We refer to [25] to see that the commutativity of the diagram involving the functional and the discrete spaces holds in the high order case. Some nice properties characterize the square matrix \mathbf{V}^p of size m which depends on the values of p , r and d .

Property 1 The entries of \mathbf{V}^p can be computed (on the paper) by combinatorial formula and do not depend on the metric of the simplex v for which they are calculated.

Dofs are normalized. As an example, for $p = 1$, the $\sigma_i(\mathbf{w}_j)$ are integrals of terms as $\lambda^{\mathbf{k}} \nabla \lambda_{n_i} \cdot \mathbf{t}_e$ (where $\lambda^{\mathbf{k}}$ has to be intended as explained in Def. 3, involving the barycentric coordinates appearing in \mathbf{w}_j and in the polynomial of the moment σ_i , and \mathbf{t}_e stands also for $\mathbf{t}_{f,i}, \mathbf{t}_{v,i}$). It can be shown that $\nabla \lambda_{n_i} \cdot \mathbf{t}_e = -1$ (resp. $+1$) if, w.r.t. the orientation of e , n_i is the first (resp. second) endpoint of e , and 0 if n_i is not an endpoint of e ; the only terms that remain in the integral are of the type $\lambda^{\mathbf{k}}$, therefore $\sigma_i(\mathbf{w}_j)$ can be calculated using the well-known formula (see for instance [23] for a proof): For any multi-index $\mathbf{k} \in \mathcal{I}(p' + 1, k)$ and p' -simplex s , $p' > 0$, we have

$$\frac{1}{|s|} \int_s \lambda_s^{\mathbf{k}} = (p')! (k_1! k_2! \dots k_{p'+1}!) / (p' + k)!,$$

with $\lambda_s^{\mathbf{k}}$ as in (2). This value is clearly independent of the metric of s . The independence from the metric of the p' -face s of v for which they are calculated means that the entries of \mathbf{V}^p can be computed *once* on a generic volume v and are valid in any other volume v' different from v , up to a suitable orientation of the edges and choice of independent sides in v' . For a quicker and precise calculation, high order quadrature formula [29] can also be used.

Property 2 The matrix \mathbf{V}^p is block triangular ($p < 3$).

The matrix \mathbf{V}^p can be written in a block lower triangular form, if dofs, indexing the rows i , and generators, indexing the columns j , are suitably numbered. On the one hand, dofs can be ordered block-wisely, depending on the dimension p' of their support (domain of integration), from the lowest allowed ($p' = p$) to the highest one (which depends also on the degree r). On the other hand, the set \mathcal{B} of generators $\lambda^{\mathbf{k}}\mathbf{w}^s$ (with s a p -simplex) for $W_{h,r}^p$ stated in Definition 4 can be listed, in each volume, as follows: case (1), those with the barycentric coordinates in $\lambda^{\mathbf{k}}$ and \mathbf{w}^s all associated with all the vertices of s ; case (ℓ), $2 < \ell \leq \bar{\ell}$, with the upper bound $\bar{\ell}$ which depends on r and is limited by the value $(d+1-p)$, those with the barycentric coordinates in $\lambda^{\mathbf{k}}$ and \mathbf{w}^s all associated with all the vertices of a $(p+\ell-1)$ -simplex whose boundary contains s .

Let us denote by \bar{p} the maximal dimension, allowed by the considered r , of the domain of integration in the definition of dofs for $W_{h,r}^p(v)$. The order we adopt to list the generators in \mathcal{B} thus yields, in each volume, subsets \mathcal{B}_g , $p \leq g \leq \bar{p} \leq d$, such that functions in \mathcal{B}_g are characterized by moments (dofs) equal to 0 on p' -simplices with $p' < g$. Namely, the order we adopt to list the generators in \mathcal{B} follows the order dictated by increasing the dimension of the support of dofs, which is exactly the one we use to list dofs into blocks. We thus may use a unique array of integers to list (thus to order) both dofs and generators. Following this order, the matrix \mathbf{V}^p with entries $(\mathbf{V}^p)_{ij} = \sigma_i(\mathbf{w}_j)$ is block triangular.

Property 3 Matrix \mathbf{V}^p is computationally cheap to invert.

Lagrange interpolation on uniformly distributed points is not stable w.r.t the order. This fact occurs in the present construction since the generators are indexed on the basis of the FE principal lattice of order r and yields to ill-conditioned matrices \mathbf{V}^p . In the present case, the blocks on the diagonal of \mathbf{V}^p are Toeplitz matrices of size, say, $m_b \geq 1$, thus invertible in $O(m_b^2)$ operations. Moreover, the matrix \mathbf{V}^p has a block-structure that can be defined recursively³, depending on d , p and r , as it can

³ Let us consider the square matrices \mathbf{A}_m , $m \geq 0$, defined recursively as follows:

$$\mathbf{A}_0 = \mathbf{A}, \quad \mathbf{A}_m = \begin{pmatrix} \mathbf{A}_{m-1} & \mathbf{0} \\ \mathbf{B}_m & \mathbf{C}_m \end{pmatrix}, \quad m \geq 1,$$

where the rectangular matrices \mathbf{B}_m and the square matrices \mathbf{C}_m , $m \geq 1$, have entries and sizes which vary with m . The construction of the square matrix \mathbf{V}^p of size $\dim(W_{h,r}^p(v))$, for a suitable ordering of the dofs σ_i (and thus of the generators \mathbf{w}_j) depending on d , p and r , is similar, in terms of structure, to that of the matrix \mathbf{A}_m . In \mathbf{V}^p , the starting matrix \mathbf{A} is block diagonal, with diagonal blocks of size m_b that are Toeplitz matrices. The difference with \mathbf{A}_m is that in the matrix \mathbf{V}^p , for a fixed $p < 3$ and d , when we pass from r (m) to $r+1$ ($m+1$), we do not have exactly the block \mathbf{A}_{m-1} but a modified one, say $\tilde{\mathbf{A}}_{m-1}$, with different entries and larger size. To see this fact, just compare, for example, the matrices \mathbf{V}^1 one would have for $r=1$ and for $r=2$ when $d=2$. If $r=1$, then \mathbf{V}^1 is the identity matrix of size 3 (in this case, $m_b=1$). If $r=2$, the matrix \mathbf{V}^1 is given in Example 2: we may remark that the block-diagonal part of \mathbf{V}^1 has now size 6 (here, $m_b=2$) with entries no more equal to 1.

be seen from the Examples 1,2,3 below. Its inverse can also be computed recursively⁴. Moreover, due to the independence of \mathbf{V}^p from the metric in v , the inverse $(\mathbf{V}^p)^{-1}$ has to be computed only once for all the mesh volumes.

Property 4 The entries of the matrix $(\mathbf{V}^p)^{-1}$ are integer numbers.

This is related to the meaning of the entries of $(\mathbf{V}^p)^{-1}$, to the considered generators, relying on linear combinations of products $\lambda^{\mathbf{k}} \nabla \lambda_i$, with \mathbf{k} a multi-index and λ_i a barycentric coordinate, and to the considered moments, integrals over *entire* simplices of dimension $0 \leq p' \leq d$ (with dofs on small-simplices, the entries of $(\mathbf{V}^p)^{-1}$ are not integers, indeed small-simplices are *portions* of mesh (big) simplices). We recall the double aspect of Whitney forms, with the considered generators as proxies: the weights (dofs, here moments) of Whitney forms that allow to represent a p -manifold as a p -chain (linear combination of p -simplices) are the same as the weights that represent a p -form by a p -cochain. We are thus looking for the coefficients of linear combinations of generators, thus of linear combinations of p' -simplices, that make moments on them be in duality with generators. In other words, we look for p' -chains built on entire p' -simplices of the volume, not portions of them, such that moments on them applied to field generators, give 1 or 0. The coefficients in these p' -chains are the entries of $(\mathbf{V}^p)^{-1}$. Property (iv) is one of the most interesting aspects of the present construction.

In the following examples, we detail dofs and generators for fields in $W_{h,r}^p$ together with the matrix \mathbf{V}^p and its inverse for some values of d , p and r .

Example 1 [$d = 2$, $p = 0$, $r = 2$]

Let us consider a face $f = \{n_1, n_2, n_3\}$. Dofs $\{\sigma_i\}$ for fields $z \in W_{h,2}^0(f)$ are defined by relying on Definition 5 and read

$$\begin{aligned} \{\sigma_1(z) = z(n_1), \quad \sigma_2(z) = z(n_2), \quad \sigma_3(z) = z(n_3), \\ \sigma_4(z) = \frac{1}{|e_{12}|} \int_{e_{12}} z, \quad \sigma_5(z) = \frac{1}{|e_{23}|} \int_{e_{23}} z, \quad \sigma_6(z) = \frac{1}{|e_{13}|} \int_{e_{13}} z\} \end{aligned}$$

with $\mathbf{t}_{ij} = \mathbf{x}_j - \mathbf{x}_i$ and $|e_{ij}| = |\mathbf{t}_{ij}|$ the Riemann measure of the side with vertices n_i, n_j . With the set of dofs we may associate a *listing array*, here [1 1; 2 2; 3 3; 1 2; 2 3; 1 3], if we adopt indices [i i] to refer to σ_i , $i = 1, 3$, and [i j] to indicate the dof involving the integral on the side e_{ij} . The generators $\{w_j\}$ of $W_{h,2}^0(f)$ can be listed by relying on the listing array of dofs: indeed, they are

$$\begin{aligned} \{w_1 = \lambda_1 \lambda_1, \quad w_2 = \lambda_2 \lambda_2, \quad w_3 = \lambda_3 \lambda_3, \\ w_4 = \lambda_1 \lambda_2, \quad w_5 = \lambda_2 \lambda_3, \quad w_6 = \lambda_1 \lambda_3\}, \end{aligned}$$

⁴ The inverse $(\mathbf{A}_m)^{-1}$, $m \geq 0$, can be defined recursively as follows:

$$(\mathbf{A}_0)^{-1} = \mathbf{A}^{-1}, \quad (\mathbf{A}_m)^{-1} = \begin{pmatrix} (\mathbf{A}_{m-1})^{-1} & \mathbf{0} \\ -(\mathbf{C}_m)^{-1} \mathbf{B}_m (\mathbf{A}_{m-1})^{-1} & (\mathbf{C}_m)^{-1} \end{pmatrix}, \quad m \geq 1.$$

The computation of $(\mathbf{V}^p)^{-1}$ is algorithmically similar to that of $(\mathbf{A}_m)^{-1}$.

where λ_j stands for λ_{n_j} . The matrices $(\mathbf{V}^0)^t$ and $(\mathbf{V}^0)^{-1}$ read

$$(\mathbf{V}^0)^t = \frac{1}{6} \begin{pmatrix} 6 & 0 & 0 & 2 & 0 & 2 \\ 0 & 6 & 0 & 2 & 2 & 0 \\ 0 & 0 & 6 & 0 & 2 & 2 \\ 0 & 0 & 0 & 1 & 0 & 0 \\ 0 & 0 & 0 & 0 & 1 & 0 \\ 0 & 0 & 0 & 0 & 0 & 1 \end{pmatrix}, \quad (\mathbf{V}^0)^{-1} = \begin{pmatrix} 1 & 0 & 0 & 0 & 0 & 0 \\ 0 & 1 & 0 & 0 & 0 & 0 \\ 0 & 0 & 1 & 0 & 0 & 0 \\ -2 & -2 & 0 & 6 & 0 & 0 \\ 0 & -2 & -2 & 0 & 6 & 0 \\ -2 & 0 & -2 & 0 & 0 & 6 \end{pmatrix}.$$

Example 2 [$d = 2, p = 1, r = 2$]

Let us consider a face $f = \{n_1, n_2, n_3\}$. Dofs $\{\sigma_i\}$ for fields $\mathbf{z} \in W_{h,2}^1(f)$ are defined by relying on Definition 6 and Proposition 3 for face dofs, with $\mathbf{t}_{12} = \mathbf{x}_2 - \mathbf{x}_1$ and $\mathbf{t}_{13} = \mathbf{x}_3 - \mathbf{x}_1$ playing the role of “two independent sides” on that face, and read

$$\begin{aligned} \{\sigma_1(\mathbf{z}) &= \frac{1}{|e_{12}|} \int_{e_{12}} (\mathbf{z} \cdot \mathbf{t}_{12}) \lambda_1, & \sigma_2(\mathbf{z}) &= \frac{1}{|e_{12}|} \int_{e_{12}} (\mathbf{z} \cdot \mathbf{t}_{12}) \lambda_2, \\ \sigma_3(\mathbf{z}) &= \frac{1}{|e_{13}|} \int_{e_{13}} (\mathbf{z} \cdot \mathbf{t}_{13}) \lambda_1, & \sigma_4(\mathbf{z}) &= \frac{1}{|e_{13}|} \int_{e_{13}} (\mathbf{z} \cdot \mathbf{t}_{13}) \lambda_3, \\ \sigma_5(\mathbf{z}) &= \frac{1}{|e_{23}|} \int_{e_{23}} (\mathbf{z} \cdot \mathbf{t}_{23}) \lambda_2, & \sigma_6(\mathbf{z}) &= \frac{1}{|e_{23}|} \int_{e_{23}} (\mathbf{z} \cdot \mathbf{t}_{23}) \lambda_3, \\ \sigma_7(\mathbf{z}) &= \frac{1}{|f|} \int_f \mathbf{z} \cdot \mathbf{t}_{12}, & \sigma_8(\mathbf{z}) &= \frac{1}{|f|} \int_f \mathbf{z} \cdot \mathbf{t}_{13}. \end{aligned}$$

Right above, $|e_{ij}|$ (resp. $|f|$) stands for the Riemann measure of the side (resp. face) with vertices n_i, n_j (resp. n_1, n_2, n_3). With the set of dofs we may associate the *listing array* [1 1 2; 2 1 2; 1 1 3; 3 1 3; 2 2 3; 3 2 3; 3 1 2; 2 1 3], if we adopt indices [i i j] (resp. [j i j]) for the dof involving the integral of $(\cdot)\lambda_i$ (resp. $(\cdot)\lambda_j$) on the side e_{ij} , and [i j 1] to indicate the dof involving the integral of $\mathbf{z} \cdot \mathbf{t}_{j1}$ on f . The generators $\{\mathbf{w}_j\}$ of $W_{h,2}^1(f)$ can be listed by relying on the listing array of dofs: indeed, they are

$$\begin{aligned} \{\mathbf{w}_1 &= \lambda_1 \mathbf{w}^{12}, & \mathbf{w}_2 &= \lambda_2 \mathbf{w}^{12}, & \mathbf{w}_3 &= \lambda_1 \mathbf{w}^{13}, & \mathbf{w}_4 &= \lambda_3 \mathbf{w}^{13}, \\ \mathbf{w}_5 &= \lambda_2 \mathbf{w}^{23}, & \mathbf{w}_6 &= \lambda_3 \mathbf{w}^{23}, & \mathbf{w}_7 &= \lambda_3 \mathbf{w}^{12}, & \mathbf{w}_8 &= \lambda_2 \mathbf{w}^{13}\}. \end{aligned}$$

Note that, by following the listing array of dofs, we do not consider the generator $\lambda_1 \mathbf{w}^{23}$, which is indeed redundant, in the sens of Proposition 2, if considered together with \mathbf{w}_7 and \mathbf{w}_8 . The matrices $(\mathbf{V}^1)^t$ and $(\mathbf{V}^1)^{-1}$ read

$$(\mathbf{V}^1)^t = \frac{1}{12} \begin{pmatrix} 4 & 2 & 0 & 0 & 0 & 0 & 3 & 1 \\ 2 & 4 & 0 & 0 & 0 & 0 & 3 & 2 \\ 0 & 0 & 4 & 2 & 0 & 0 & 1 & 3 \\ 0 & 0 & 2 & 4 & 0 & 0 & 2 & 3 \\ 0 & 0 & 0 & 0 & 4 & 2 & -1 & 2 \\ 0 & 0 & 0 & 0 & 2 & 4 & -2 & 1 \\ 0 & 0 & 0 & 0 & 0 & 0 & 2 & 1 \\ 0 & 0 & 0 & 0 & 0 & 0 & 1 & 2 \end{pmatrix}, \quad (\mathbf{V}^1)^{-1} = \begin{pmatrix} 4 & -2 & 0 & 0 & 0 & 0 & 0 & 0 \\ -2 & 4 & 0 & 0 & 0 & 0 & 0 & 0 \\ 0 & 0 & 4 & -2 & 0 & 0 & 0 & 0 \\ 0 & 0 & -2 & 4 & 0 & 0 & 0 & 0 \\ 0 & 0 & 0 & 0 & 4 & -2 & 0 & 0 \\ 0 & 0 & 0 & 0 & -2 & 4 & 0 & 0 \\ -4 & -2 & 2 & -2 & 2 & 4 & 8 & -4 \\ 2 & -2 & -4 & -2 & -4 & -2 & -4 & 8 \end{pmatrix}.$$

Example 3 [$d = 3, p = 2, r = 2$]

Let us consider the volume $v = \{n_1, n_2, n_3, n_4\}$. Dofs $\{\sigma_i\}$ for fields in $\mathbf{z} \in W_{h,2}^2(v)$ are defined by relying on Definition 7 and Propositions 5, 6, resp., for face and volume

$$(\mathbf{V}^2)^{-1} = \begin{pmatrix} -18 & 6 & 6 & 0 & 0 & 0 & 0 & 0 & 0 & 0 & 0 & 0 & 0 & 0 & 0 \\ 6 & -18 & 6 & 0 & 0 & 0 & 0 & 0 & 0 & 0 & 0 & 0 & 0 & 0 & 0 \\ 6 & 6 & -18 & 0 & 0 & 0 & 0 & 0 & 0 & 0 & 0 & 0 & 0 & 0 & 0 \\ 0 & 0 & 0 & 18 & -6 & -6 & 0 & 0 & 0 & 0 & 0 & 0 & 0 & 0 & 0 \\ 0 & 0 & 0 & -6 & 18 & -6 & 0 & 0 & 0 & 0 & 0 & 0 & 0 & 0 & 0 \\ 0 & 0 & 0 & -6 & -6 & 18 & 0 & 0 & 0 & 0 & 0 & 0 & 0 & 0 & 0 \\ 0 & 0 & 0 & 0 & 0 & 0 & -18 & 6 & 6 & 0 & 0 & 0 & 0 & 0 & 0 \\ 0 & 0 & 0 & 0 & 0 & 0 & 6 & -18 & 6 & 0 & 0 & 0 & 0 & 0 & 0 \\ 0 & 0 & 0 & 0 & 0 & 0 & 0 & 0 & 0 & 18 & -6 & -6 & 0 & 0 & 0 \\ 0 & 0 & 0 & 0 & 0 & 0 & 0 & 0 & 0 & -6 & 18 & -6 & 0 & 0 & 0 \\ 0 & 0 & 0 & 0 & 0 & 0 & 0 & 0 & 0 & -6 & -6 & 18 & 0 & 0 & 0 \\ 6 & 6 & 12 & -6 & 0 & 6 & -6 & 0 & 6 & -12 & -6 & -6 & 10 & 10 & 5 \\ 6 & 0 & -6 & -6 & -6 & -12 & 0 & 6 & -6 & 6 & 12 & 6 & -5 & 5 & 0 \\ 0 & -6 & 6 & 0 & -6 & 6 & 6 & 6 & 12 & -6 & -6 & -12 & 5 & -5 & -5 \end{pmatrix}.$$

Example 4 [$d = 3, p = 3, r = 1$]

Let us consider the volume $v = \{n_1, n_2, n_3, n_4\}$. Dofs $\{\sigma_i\}$ for fields $z \in W_{h,1}^3(v)$ are defined by relying on Definition 8, and read

$$\{\sigma_1(z) = \int_v z \lambda_1, \quad \sigma_2(z) = \int_v z \lambda_2, \quad \sigma_3(z) = \int_v z \lambda_3, \quad \sigma_4(z) = \int_v z \lambda_4\}.$$

With the set of dofs we may associate the *listing array* [1 1 2 3 4; 2 1 2 3 4; 3 1 2 3 4; 4 1 2 3 4] if we adopt indices [i i j 1 m] (resp., [j i j 1 m], [1 i j 1 m], [m i j 1 m]) to indicate the dof involving the integral of $z \lambda_i$ (resp., $z \lambda_j, z \lambda_1, z \lambda_m$) on the volume v . The generators $\{w_j\}$ of $W_{h,1}^3(v)$ can be listed by relying on the listing array of dofs: indeed, they are

$$\{w_1 = \lambda_1 w^v, \quad w_2 = \lambda_2 w^v, \quad w_3 = \lambda_3 w^v, \quad w_4 = \lambda_4 w^v\}.$$

The matrices $(\mathbf{V}^3)^t$ and $(\mathbf{V}^3)^{-1}$ read

$$(\mathbf{V}^3)^t = \frac{1}{20} \begin{pmatrix} 2 & 1 & 1 & 1 \\ 1 & 2 & 1 & 1 \\ 1 & 1 & 2 & 1 \\ 1 & 1 & 1 & 2 \end{pmatrix}, \quad (\mathbf{V}^3)^{-1} = \begin{pmatrix} 16 & -4 & -4 & -4 \\ -4 & 16 & -4 & -4 \\ -4 & -4 & 16 & -4 \\ -4 & -4 & -4 & 16 \end{pmatrix}.$$

6 Numerical results for high order edge elements

In this section, we test the performances of the proposed high order edge elements, by solving a simple but delicate problem of the empty cavity resonator in two dimensions. Given a bounded domain $\Omega \in \mathbb{R}^2$ with connected boundary Γ , we seek scalars ω^2 and non-trivial (*i.e.* not identically zero) electric fields \mathbf{u} satisfying

$$\begin{aligned} \nabla \times \left(\frac{1}{\mu} \nabla \times \mathbf{u} \right) - \omega^2 \epsilon \mathbf{u} &= 0 && \text{in } \Omega, \\ \nabla \cdot (\epsilon \mathbf{u}) &= 0 && \text{in } \Omega, \\ \mathbf{t} \cdot \mathbf{u} &= 0 && \text{on } \Gamma, \end{aligned} \tag{20}$$

ω^2	degree 1	degree 2	degree 3	degree 4
1.00	1.98	4.02	5.78	7.78
1.00	2.08	4.00	5.96	7.45
2.00	1.93	3.96	5.97	7.96
4.00	1.99	3.87	5.90	7.97
4.00	1.97	3.87	5.91	7.97
5.00	1.97	3.87	5.87	7.93
5.00	1.88	3.92	5.94	7.95
8.00	1.36	3.85	5.89	7.91
9.00	1.98	2.59	5.82	7.93
9.00	2.02	3.86	5.86	7.95

Table 1 Computed h -convergence rates for the edge element discretization of polynomial degree $r = 1, 2, 3, 4$ of problem (21).

with ϵ and μ the electric permittivity and the magnetic permeability, respectively, assumed to be real scalar functions satisfying $0 < \epsilon_* \leq \epsilon \leq \epsilon^*$ and $0 < \mu_* \leq \mu \leq \mu^*$ almost everywhere on Ω . As stated in [4], the variational formulation of problem (20) reads:

$$\begin{aligned} \text{find pairs } (\omega^2, \mathbf{u}) \in \mathbb{R} \times \mathbf{H}_{\text{curl},0}(\Omega), (\omega^2, \mathbf{u}) \neq (0, \mathbf{0}), \text{ such that :} \\ \int_{\Omega} \frac{1}{\mu} \nabla \times \mathbf{u} \nabla \times \mathbf{v} = \omega^2 \int_{\Omega} \epsilon \mathbf{u} \cdot \mathbf{v}, \quad \forall \mathbf{v} \in \mathbf{H}_{\text{curl},0}(\Omega), \end{aligned} \quad (21)$$

where $\mathbf{H}_{\text{curl},0}(\Omega) = \{\mathbf{u} \in \mathbf{H}_{\text{curl}}(\Omega), \mathbf{t} \cdot \mathbf{u}|_{\Gamma} = 0\}$. Note that both ω^2 and \mathbf{u} are unknowns, as is usual for eigenvalue problems. The discrete problem associated with (21) is obtained by choosing $\mathbf{v} \in W_h$, a finite-dimensional subspace of $\mathbf{H}_{\text{curl},0}(\Omega)$. Here, $W_h = \{\mathbf{v}_h \in \mathbf{H}_{\text{curl},0}(\Omega), (\mathbf{v}_h)|_v \in W_{h,r}^1(v), \forall v \in \mathcal{T}\}$, with $W_{h,r}^1(v)$ the space generated by the functions given in Definition 4 ($p = 1, r \geq 1$). The considered domain and parameters are $\Omega = [0, \pi]^2$ and $\epsilon = \mu = 1$. In this case it is easy to find the exact eigenvalues of problem (20), which are given by $0 \neq \omega^2 = n^2 + m^2$, with $n, m = 0, 1, \dots$. Numerical computations for the Maxwell eigenvalues are based on the use of the routine DGEGV of the Lapack library.

The h -convergence analysis for the Maxwell eigenvalue problem is done by a simplicial finite element code based on Whitney edge elements of polynomial degree $r = 1, 2, 3, 4$. We choose structured regular meshes of four different sizes: $h \in \{\frac{\pi}{15}, \frac{\pi}{12}, \frac{\pi}{9}, \frac{\pi}{6}\}$. Table 1 contains the computed rates of the h -convergence curves of the error $|\omega^2 - \omega_h^2|$ for the first ten eigenvalues when edge elements of different polynomial degree r are used. Convergence with a rate $O(h^{2r})$ is observed, in agreement with the theoretical result of Theorems 4.4 and 5.4 in [4]. Fig. 3 and 4 show the log-plots of the error $|\omega^2 - \omega_h^2|$ as a function of the mesh size h .

We now turn to the r -convergence analysis for the Maxwell eigenvalue problem. The question is whether or not we achieve exponential convergence when computing Maxwell eigenvalues ω^2 . That is to say, a bound for the relative error dependent on

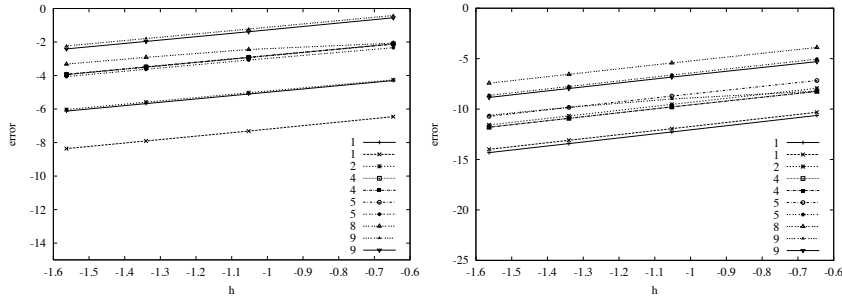


Fig. 3 h -convergence for the error for the first (left) and second (right) order edge element approximation for Dirichlet boundary conditions.

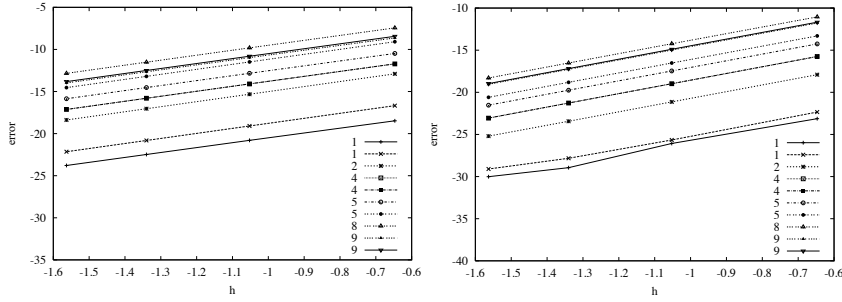


Fig. 4 h -convergence for the error for the third (left) and fourth (right) order edge element approximation for Dirichlet boundary conditions.

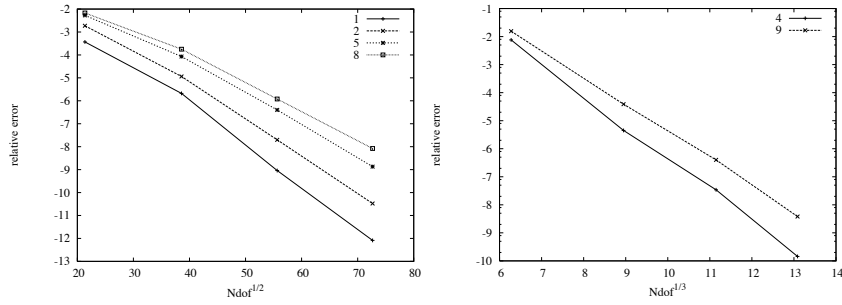


Fig. 5 r -convergence for the relative error for the Maxwell eigenvalues on the second mesh plotted with $N\text{dof}^{1/2}$ (left) and $N\text{dof}^{1/3}$ (right).

the number of degrees of freedom ($N\text{dof}$) is given by

$$\delta = \frac{|\omega^2 - \omega_h^2|}{\omega^2} \leq C \exp(-b N\text{dof}^\alpha), \quad (22)$$

where the positive constants C , α and b are independent of $N\text{dof}$. Estimate (22) was established in [2] for the discretized electric field on two-dimensional polygonal domains where $\alpha = 1/2$ when the solution is smooth and $\alpha = 1/3$ when the solution is singular

(see also [11] for a large variety of numerical tests). In the computation of Maxwell eigenvalues for the considered case, numerical results by the proposed method show an exponential rate of convergence with respect to the approximation polynomial degree r . We report in (23) the computed values for the constant α appearing in the bound (22) when the approximated Maxwell eigenvalues ω_h are computed by the proposed edge elements of degree $r = 1, 2, 3, 4$ on the second mesh ($h = \frac{\pi}{12}$):

$$\begin{array}{cccccccccc} \omega^2 & 1. & 1. & 2. & 4. & 4. & 5. & 5. & 8. & 9. & 9. \\ \alpha & 0.46 & 0.74 & 0.67 & 0.23 & 0.23 & 0.32 & 0.72 & 0.73 & 0.37 & 0.30 \end{array} \quad (23)$$

These values are obtained by means of the so-called Golden Section Search in One Dimension algorithm [21] applied to minimize over a real interval the quadratic function $F(\alpha) = \sum_{r=1}^4 ((\delta)_r - Ce^{-b(\text{Ndof}_r)^\alpha})^2$, where $(\delta)_r$ (resp. Ndof_r) denotes the relative error on ω^2 (resp. the corresponding Ndof) for the degree r of the edge element approximation. Here we have $(\text{Ndof}_1, \dots, \text{Ndof}_4) = (456, 1488, 3096, 5280)$. The constants C and b are computed depending on α by solving the rectangular system $\log(\delta)_r = \log(C) - b(\text{Ndof}_r)^\alpha$, for $r = 1, \dots, 4$. To confirm that exponential convergence has been obtained, a semi-log scale of the relative error for the Maxwell eigenvalues, obtained using r -refinement on the second mesh, is plotted in Fig. 5 against Ndof^α . We have chosen, for each eigenvalue ω^2 , the theoretical α which is closer to the corresponding computed one given in (23). For example, when considering the eigenvalue 1, the computed values 0.46 or 0.74 for α are closer to $1/2$ than to $1/3$. Similarly, for the eigenvalues 2 (with 0.67), 5 (with 0.32 or 0.72) and 8 (with 0.73) we are closer to $1/2$. In a semi-log scale visualization, we observe that the curves for the eigenvalues 1, 2, 5, 8 (resp. 4, 9) are straight lines as functions of $\text{Ndof}^{1/2}$ (resp. $\text{Ndof}^{1/3}$) for approximation degrees $r > 0$. The exponential convergence rate predicted by (22) has been thus obtained.

7 Conclusions and acknowledgements

We have analyzed a friendly and effective way of defining generators and computing dofs for high order simplicial FEs in computational electromagnetism, with a detailed look at the first family of Nédélec in H_{curl} and H_{div} . If generators are listed by using the listing array built for dofs, we may avoid redundancies and end up with a basis of the discrete space. We have shown how it is possible to find new basis functions in duality with the considered dofs (moments), by considering suitable linear combinations (with integer coefficients) of the proposed generators. Some examples are given in Section 5, where functions and dofs are listed explicitly. Two points are important. First, the fact of working with scalar or vector fields expressed only in barycentric coordinates: it allows to define quantities locally in each tetrahedron of the mesh and to easily solve problems associated with the (inner) orientation of simplices, at the matrix/vector FE assembling step. Second, the considered generators are associated with a geometrical

construction (that of the small p -simplices in each mesh tetrahedron v), in the spirit of Whitney forms: given one of the generators, we know immediately its “position” in the field approximation and its support in the mesh. We have presented simple numerical tests which aim at showing that the proposed basis functions can be used in practice. Optimal error estimates on the computation of Maxwell eigenvalues for a square domain are numerically proved. For more involved applications (L-shaped domains, discontinuous coefficients, 3D concrete problems), the preconditioning issue is under study. The first author is grateful to the French National Research Agency (ANR) which finances her PhD in the framework of the project MEDIMAX, ANR-13-MONU-0012. The second author warmly thanks the CASTOR team at INRIA Sophia-Antipolis for the delegation in 2015, during which this work was completed, and is grateful to Alexandre Ern for stimulating conversations on finite elements during his visits to the Jean-Alexandre Dieudonné Laboratory in Nice.

References

1. M. Ainsworth, J. Coyle, Hierarchic finite element bases on unstructured tetrahedral meshes, *Int. J. Numer. Meth. Engr.*, 58/14 (2003) 2103-2130.
2. M. Ainsworth, K. Pinchedez, hp -approximations theory for BDFM/RT finite elements and applications, *SIAM J. Numer. Anal.*, 40 (2003) 2047-2068.
3. D. Arnold, R. Falk, R. Winther, Finite element exterior calculus, homological techniques, and applications, *Acta Numerica*, 15 (2006) 1-155.
4. D. Boffi, F. Fernandes, L. Gastaldi, I. Perugia, Computational models of electromagnetic resonators: analysis of edge element approximation, *SIAM J. Numer. Anal.*, 36 (1999) 1264-1290.
5. A. Bossavit, On finite elements for the electricity equation, in *The Mathematics of Finite Elements*, J.R. Whiteman ed., Academic Press, London (1982) 85-92.
6. A. Bossavit, *Computational Electromagnetism*, Academic Press Inc., San Diego, CA, 1998. Variational formulations, complementarity, edge elements.
7. A. Bossavit, Generating Whitney forms of polynomial degree one and higher, *IEEE Trans. Magn.*, 38/2 (2002) 341-344.
8. A. Bossavit, F. Rapetti, Whitney elements, from Manifolds to Fields, in “Spectral and high order methods for PDEs”, M. Azaiez, H. El Fekihand, J.S. Hestaven eds., *ICOSAHOM 12* procs., LNCSE Vol. 95, pp. 179-189, Springer-Verlag, 2014.
9. S. H. Christiansen, F. Rapetti, On high order finite element spaces of differential forms, *Mathematics of Computation*, 85/298 (2016) 517-548, 2016.
10. P.G. Ciarlet, *The Finite Element Method for Elliptic Problems*, North-Holland, Amsterdam (1978).
11. J. Coyle, P.D. Ledger, Evidence of exponential convergence in the computation of Maxwell eigenvalues, *Comp. Meth. Appl. Mech. Engng.* 194/2 (2005) 587-604.
12. A. Ern, J.-L. Guermond, Finite element quasi-interpolation and best approximation, 2015, arXiv:1505.06931 [math.NA].
13. F. Fuentes, B. Keith, L. Demkowicz, S. Nagaraj, Orientation embedded high order shape functions for the exact sequence elements of all shapes, *Computers & Mathematics with applications* 70/4 (2015) 353-458.
14. J. Gopalakrishnan, L.E. Garcia-Castillo, L.F. Demkowicz, Nédélec spaces in affine coordinates, *ICES Report no. 03-48* (2003).

15. R. Hiptmair. Canonical construction of finite elements. *Math. Comp.*, 68/228 (1999) 1325-1346.
16. R. Hiptmair. Finite elements in computational electromagnetism. *Acta Numer.*, 11 (2002) 237-339.
17. G. Karniadakis, S. Sherwin, *Spectral/hp Element Methods for CFD*, Oxford University Press, Oxford (1999).
18. P. Monk, *Finite element methods for Maxwells equations*, Numerical Mathematics and Scientific Computation. Oxford University Press, New York (2003).
19. J.C. Nédélec, Mixed finite elements in \mathbb{R}^3 , *Numer. Math.*, 35/2 (1980) 315-341.
20. J.C. Nédélec, A new family of mixed finite elements in \mathbb{R}^3 , *Numer. Math.*, 50/1 (1986) 57-81.
21. W. H. Press, S. A. Teukolsky, W. T. Vetterling, B. P. Flannery, *Numerical Recipes: The Art of Scientific Computing*, Cambridge University Press (2007).
22. A. Quarteroni, A. Valli, *Numerical Approximation of Partial Differentials Equations*, Springer (2008).
23. F. Rapetti, High order edge elements on simplicial meshes, *Meth. Math. en Anal. Num.*, 41/6 (2007) 1001-1020.
24. F. Rapetti, A. Bossavit, Geometrical localization of the degrees of freedom for Whitney elements of higher order, Special Issue on "Computational Electromagnetism", *IEE Proc. Science, Measurement and Technology*, 1/1 (2007) 63-66.
25. F. Rapetti, A. Bossavit, Whitney forms of higher degree, *SIAM J. on Numerical Analysis*, 47/3 (2009) 2369-2386.
26. P.A. Raviart, J.-M. Thomas, *Introduction à l'analyse numérique des équations aux dérivées partielles*, Collection Mathématiques appliquées pour la maîtrise, P.G. Ciarlet and J.-L. Lions eds., Masson (1988).
27. B. Szabo, I. Babuska, *Finite Element Analysis*, Wiley, New York (1991).
28. J. Schoberl, S. Zaglmayr, High order Nédélec elements with local complete sequence properties, *COMPEL*, 24/2 (2005) 374-384.
29. P. Solin, K. Segeth, Ivo Dolezel, *Higher-Order Finite Element Methods*, Studies in Advances Mathematics, Chapman & Hall, CRC Press Company (2003).
30. H. Whitney, *Geometric integration theory*, Princeton Univ. Press, Princeton, N. J. (1957).